HOKKAIDO UNIVERSITY

Title	Cyclin B1 mRNA translation is temporally controlled through formation and disassembly of RNA granules
Author(s)	Kotani, Tomoya; Yasuda, Kyota; Ota, Ryoma et al.
Citation	Journal of cell biology, 202(7), 1041-1055 https://doi.org/10.1083/jcb.201302139
Issue Date	2013-09-30
Doc URL	https://hdl.handle.net/2115/53576
Rights	©Kotani et al., 2013. Originally published in Journal of cell biology. doi: 10.1083/jcb.201302139
Type	journal article
File Information	1041.full.pdf

Hokkaido University Collection of Scholarly and Academic Papers : HUSCAP

Published September 23, 2013

This article has original data in the JCB Data Viewer
http://jcb-dataviewer.rupress.org/jcb/browse/6307

Cyclin B1 mRNA translation is temporally controlled through formation and disassembly of RNA granules

Tomoya Kotani,[1] Kyota Yasuda,[2] Ryoma Ota,[1] and Masakane Yamashita[1]

[1]Department of Biological Sciences, Faculty of Science, and [2]Biosystems Science Course, Graduate School of Life Science, Hokkaido University, Sapporo 060-0810, Japan

Temporal control of messenger RNA (mRNA) translation is an important mechanism for regulating cellular, neuronal, and developmental processes. However, mechanisms that coordinate timing of translational activation remain largely unresolved. Full-grown oocytes arrest meiosis at prophase I and deposit dormant mRNAs. Of these, translational control of *cyclin B1* mRNA in response to maturation-inducing hormone is important for normal progression of oocyte maturation, through which oocytes acquire fertility. In this study, we found that dormant *cyclin B1* mRNA forms granules in the cytoplasm of zebrafish and mouse oocytes. Real-time imaging of translation revealed that the granules disassemble at the time of translational activation during maturation. Formation of *cyclin B1* RNA granules requires binding of the mRNA to Pumilio1 protein and depends on actin filaments. Disruption of *cyclin B1* RNA granules accelerated the timing of their translational activation after induction of maturation, whereas stabilization hindered translational activation. Thus, our results suggest that RNA granule formation is critical for the regulation of timing of translational activation.

Introduction

Timings of translational activation of specific mRNAs are precisely controlled in germ cells, mitotically dividing cells, neurons, and embryos. This temporal control of translation plays key roles in the regulation of meiotic and mitotic cell cycle progression, neuronal plasticity, and embryonic development (Kuersten and Goodwin, 2003; Martin, 2004; de Moor et al., 2005; Malureanu et al., 2010; Novoa et al., 2010). The most extensively studied process of those driven by temporal control of translation is the meiotic cell cycle of vertebrate oocytes. In full-grown vertebrate oocytes, the meiotic cell cycle is arrested at prophase I, and dormant mRNAs required for progression of meiosis and embryogenesis are deposited. At this stage, oocytes are unable to be fertilized. In response to specific signals such as hormones, oocytes acquire fertility through progression of meiosis from prophase I to metaphase II, a process known as oocyte maturation. Dormant mRNAs stored in oocytes, such as transcripts encoding Mos, Cyclin B, and Wee1, are translated at different timings after the induction of oocyte maturation, and this ordered translation is important for the meiotic cell cycle progression (Sagata et al., 1989; Furuno et al., 1994; Nakajo et al., 2000; Hochegger et al., 2001; Gaffré et al., 2011).

At the appropriate timing after induction of oocyte maturation, oocytes activate maturation/M-phase–promoting factor (MPF), which immediately induces germinal vesicle (GV) breakdown (GVBD) followed by meiotic spindle formation and polar body extrusion. Precocious activation of MPF caused disorganized spindle formation after the induction of GVBD, indicating that the accurate timing of MPF activation is important for proper spindle formation and subsequent chromosome segregation (Kotani and Yamashita, 2002). MPF is a heterodimer that consists of a Cdc2 catalytic subunit and Cyclin B regulatory subunit. In fish and amphibians, except *Xenopus laevis*, Cyclin B protein is absent in full-grown oocytes, and the timing of MPF activation is determined by temporally controlled Cyclin B synthesis from stored mRNAs (Tanaka and Yamashita, 1995; Kondo et al., 1997, 2001; Ihara et al., 1998; Nagahama and Yamashita, 2008). Newly synthesized Cyclin B is also required for *Xenopus* oocyte maturation in the transition between meiosis I to II

Correspondence to Tomoya Kotani: tkotani@sci.hokudai.ac.jp

Abbreviations used in this paper: CPE, cytoplasmic polyadenylation element; CPEB, CPE-binding protein; CytoB, cytochalasin B; DIG, digoxigenin; EB, extraction buffer; GV, germinal vesicle; GVBD, GV breakdown; hCG, human chorionic gonadotropin; IP, immunoprecipitation; Jasp, jasplakinolide; MIH, maturation-inducing hormone; MPF, maturation/M-phase–promoting factor; PAT, poly(A) test; PBE, Pumilio-binding element; Pum1, Pumilio1; SCA, subcortical aggregate; SG, stress granule; TC, tetracysteine; TSA, tyramide signal amplification; WT, wild type.

© 2013 Kotani et al. This article is distributed under the terms of an Attribution–Noncommercial–Share Alike–No Mirror Sites license for the first six months after the publication date (see http://www.rupress.org/terms). After six months it is available under a Creative Commons License (Attribution–Noncommercial–Share Alike 3.0 Unported license, as described at http://creativecommons.org/licenses/by-nc-sa/3.0/).

Supplemental Material can be found at:
http://jcb.rupress.org/content/suppl/2013/09/17/jcb.201302139.DC1.html
Original image data can be found at:
http://jcb-dataviewer.rupress.org/jcb/browse/6307

The Rockefeller University Press $30.00
J. Cell Biol. Vol. 202 No. 7 1041–1055
www.jcb.org/cgi/doi/10.1083/jcb.201302139

THE JOURNAL OF CELL BIOLOGY

Downloaded from jcb.rupress.org on November 18, 2013

Published September 23, 2013

(Hochegger et al., 2001). Although protein synthesis is not required for GVBD in mouse oocytes (Stern et al., 1972), Cyclin B synthesis appears to increase at the time of GVBD and is required for the meiosis I to II transition (Hampl and Eppig, 1995; Polanski et al., 1998; Ledan et al., 2001). Therefore, temporal control of *cyclin B* mRNA translation is important for driving the progression of the meiotic cell cycle in vertebrate oocytes.

Temporal control of mRNA translation relies on cis-acting elements, which provide binding sites for trans-acting factors. The cis-acting element-mediated cytoplasmic polyadenylation of dormant mRNAs drives translational activation of the mRNAs (McGrew et al., 1989; Vassalli et al., 1989; Sheets et al., 1994; Stutz et al., 1998). The cytoplasmic polyadenylation element (CPE)–binding protein (CPEB) is a trans-acting factor that binds to CPEs located in the 3′UTR of specific mRNAs, including *cyclin B1* (Hake and Richter, 1994; Gebauer and Richter, 1996; de Moor and Richter, 1999; Tay et al., 2000). After induction of oocyte maturation, CPEB directs polyadenylation of CPE-containing mRNAs, leading to recruitment of these mRNAs to polysomes. However, individual mRNAs carrying CPE in their 3′UTRs are translated at different times during oocyte maturation, suggesting that other mechanisms regulate the time of translation of distinct mRNAs. Pumilio1 (Pum1) protein, a trans-acting factor binding to Pumilio-binding element (PBE), determines the timing of translational activation of *cyclin B1* mRNA in cooperation with CPEB during *Xenopus* oocyte maturation (Nakahata et al., 2001, 2003; Piqué et al., 2008; Ota et al., 2011). However, although the biochemical details have been extensively examined using *Xenopus* oocytes, the molecular and cellular mechanisms of translational repression and activation of *cyclin B1* mRNA have not been fully elucidated.

Recent studies have demonstrated that particular RNA-binding proteins promote assembly of their target mRNAs into cytoplasmic RNA granules (Parker and Sheth, 2007; Anderson and Kedersha, 2009). For example, stress granules (SGs) and processing bodies (P bodies) are distinct types of RNA granules and extensively assembled in the cytoplasm of somatic cells when translating polysomes are disassembled. These granules are thought to be sites of mRNA remodeling, storage, and decay (Sheth and Parker, 2003; Cougot et al., 2004; Kedersha et al., 2005; Franks and Lykke-Andersen, 2007). In neuronal cells, several types of RNA granules are assembled and transported to dendrites (Knowles et al., 1996; Vessey et al., 2006; Baez et al., 2011). These neuronal granules are thought to be involved in translational repression during mRNA transport. In *Caenorhabditis elegans* and *Drosophila melanogaster*, oocytes assemble several distinct types of RNA granules, which are compositionally related to P bodies (Nakamura et al., 2001; Boag et al., 2008; Lin et al., 2008; Noble et al., 2008). These germ cell granules are thought to store maternal mRNAs in a dormant state. However, although evidence suggests the involvement of RNA granules in mRNA regulation, the precise function of RNA granules remains unknown. It is still controversial whether RNA granule formation is the cause or a consequence of translational repression (Franks and Lykke-Andersen, 2008).

In this study, we found that zebrafish and mouse oocytes store dormant *cyclin B1* mRNAs as RNA granules asymmetrically distributed in the cytoplasm. These granules disassembled during oocyte maturation in both species. Because genetic, biochemical, and cell biological approaches are available for zebrafish, this model animal provides a powerful experimental system to investigate the mechanisms of translational control of maternal mRNAs. We previously reported the development of a genetic method in zebrafish, in which the translational activation of *cyclin B1* mRNA can be visualized in real time with reporter mRNA (Yasuda et al., 2010). Using this real-time imaging, we revealed that the *cyclin B1* RNA granules disassemble at the time of translational activation of the mRNA. We further found that formation of *cyclin B1* RNA granules requires binding to Pum1 and depends on actin filaments. Disruption of *cyclin B1* RNA granules resulted in precocious translational activation and acceleration of GVBD after induction of maturation. Conversely, stabilization of *cyclin B1* RNA granules hindered translational activation and GVBD. From these results, we propose that RNA granule formation is critical for the regulation of timings of translational activation in temporal control of translation. Our results also provide the first evidence that *cyclin B1* mRNA translation is temporally regulated through the formation and disassembly of RNA granules during oocyte maturation.

Results

Identification of *cyclin B1* RNA granules in zebrafish and mouse oocytes

In zebrafish oocytes, *cyclin B1* mRNA is localized at the animal polar cytoplasm beneath the micropile, a structure existing at the animal pole of fish chorion (Fig. 1, A and B; Kondo et al., 2001). The distribution of *cyclin B1* mRNA in mouse oocytes was analyzed by in situ hybridization with a tyramide signal amplification (TSA) system. Although in situ hybridization of mouse *cyclin B1* mRNA was previously performed (Chapman and Wolgemuth, 1992) and showed distribution of the mRNA throughout the cytoplasm, we thought that the TSA system could uncover the precise distribution of the mRNA as in mRNAs in *Drosophila* embryos (Lécuyer et al., 2007). As expected, in situ hybridization with the TSA system revealed an asymmetrical distribution of *cyclin B1* mRNA in the cytoplasm of mouse oocytes (Fig. 1 C). In contrast, *α-tubulin* mRNA was detected uniformly in the cytoplasm (Fig. S1, A and B).

A recent study showed formation of Dcp1 protein particles, one of the P-body components, in the cytoplasm of mouse oocytes, suggesting RNA granule formation related to P bodies (Swetloff et al., 2009). To determine whether mouse and zebrafish oocytes store dormant mRNAs as granules, we further analyzed the distribution of *cyclin B1* mRNA by FISH. The FISH analyses revealed the existence of a large number of *cyclin B1* RNA granules in the animal polar cytoplasm beneath the micropile of zebrafish oocytes (Fig. 1, D and E; and Fig. S1, C and D). *cyclin B1* RNA granules were also detected in the cytoplasm of mouse oocytes, in which the granules were asymmetrically distributed (Fig. 1, F–H; Fig. 2 A; and Fig. S1, E–G). In contrast, *α-tubulin* mRNA was diffusely distributed throughout the oocyte cytoplasm (Fig. S1 H). Therefore, we conclude that zebrafish and mouse oocytes deposit dormant *cyclin B1* mRNA as

Downloaded from jcb.rupress.org on November 18, 2013

Published September 23, 2013

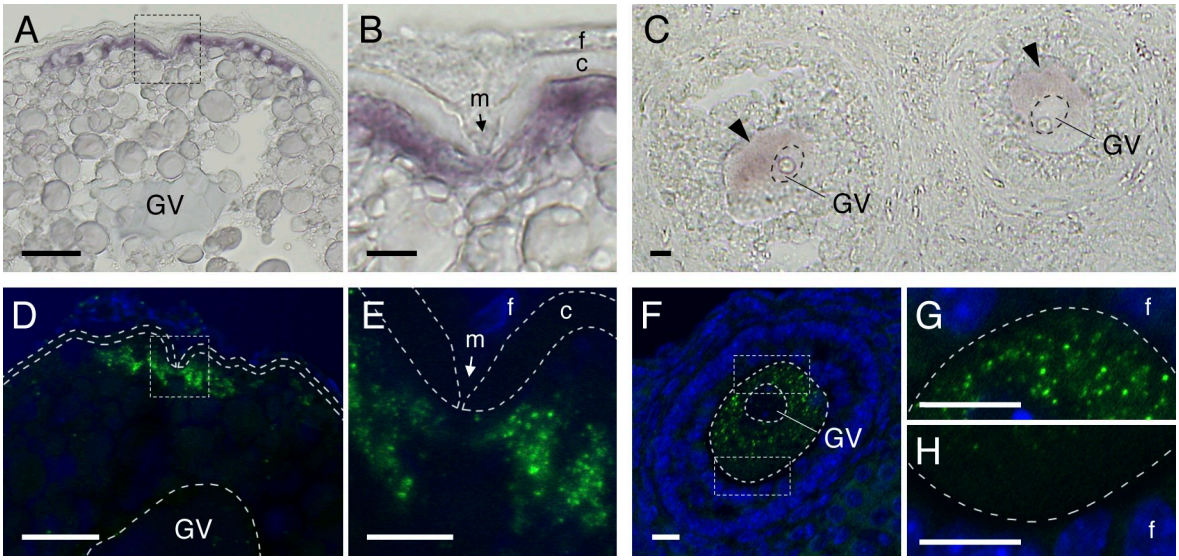


Figure 1. **Zebrafish and mouse oocytes store dormant *cyclin B1* mRNAs as asymmetrically distributed RNA granules.** (A and B) Distribution of *cyclin B1* mRNA in the zebrafish oocyte. B is an enlarged view of the boxed region in A. GV, germinal vesicle; m, micropile; f, follicle cells; c, chorion. (C) Distribution of *cyclin B1* mRNA (arrowheads) in the mouse oocyte. (D and E) FISH analysis of *cyclin B1* mRNA (green) in the zebrafish oocyte. DNA is shown in blue. E is an enlarged view of the boxed region in D. The chorion is outlined by broken lines. (F–H) FISH analysis of *cyclin B1* mRNA in the mouse oocyte. G and H are enlarged views of the boxed regions in F. The oocyte is outlined by broken lines. Bars: (A and D) 50 µm; (B, C, and E–H) 10 µm.

localized RNA granules. These results also provide the first evidence for molecular asymmetry of the full-grown mouse oocyte. We further found that *cyclin B1* RNA granules are colocalized with HuR protein, one of the SG components (Fig. S1, I and J; Gallouzi et al., 2000), suggesting that these granules are compositionally related to SGs.

Disassembly of *cyclin B1* RNA granules during oocyte maturation

To assess the relationship between RNA granule formation and translational control of *cyclin B1* mRNA, we then performed FISH analyses of oocytes at different timings after induction of oocyte maturation. Oocyte maturation in mice was induced by injection of human chorionic gonadotropin (hCG) into females 48 h after injection of pregnant mare serum gonadotropin. Dense *cyclin B1* RNA granules (21–40/100 µm^2) were detected in GV-stage oocytes (Fig. 2, A and D). The number of granules was decreased in prometaphase I (2–20/100 µm^2; 4 h after induction of maturation; Fig. 2, B and D), and the granules had almost completely disappeared in metaphase II (~1/100 µm^2; 14 h after induction of maturation; Fig. 2, C and D). The amounts of *cyclin B1* mRNA were not reduced in matured oocytes (Fig. 2 E). Therefore, the decrease in the number of granules during oocyte maturation is caused by granule disassembly, not by mRNA

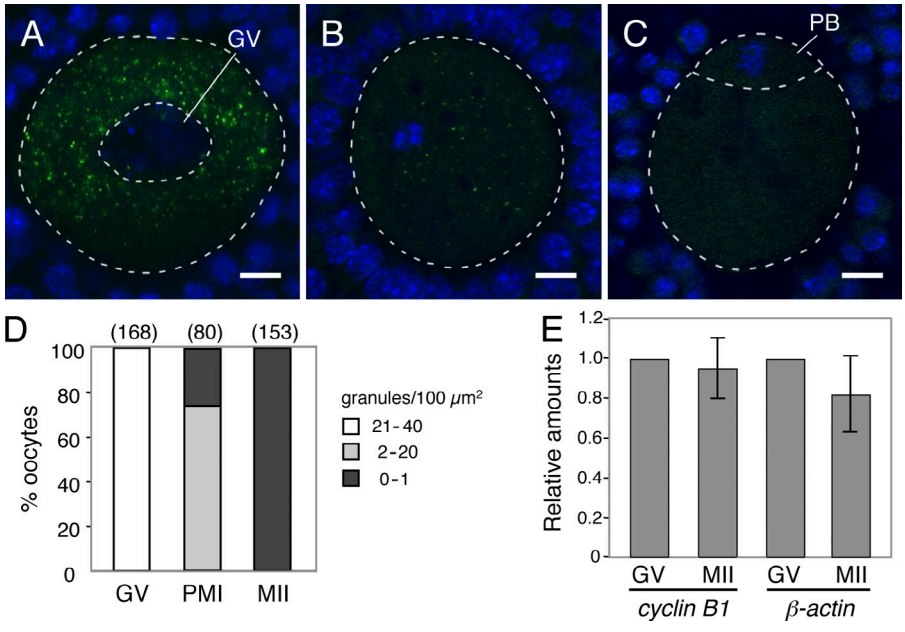


Figure 2. **Mouse *cyclin B1* RNA granules disassemble during oocyte maturation.** (A–C) FISH analysis of *cyclin B1* mRNA (green) in mouse oocytes in GV stage (A), prometaphase I (B), and metaphase II (C). DNA is shown in blue. Oocytes are outlined by broken lines. GV, germinal vesicle; PB, polar body. Bars, 10 µm. (D) The number of RNA granules per 100 µm^2 in individual oocytes in GV stage (GV), prometaphase I (PMI), and metaphase II (MII) was counted and categorized as dense (21–40), partially disassembled (2–20), and disassembled (0–1). The numbers in parentheses indicate the total number of oocytes analyzed. Similar results were obtained from two independent experiments. (E) *cyclin B1* and *β-actin* mRNAs from equal numbers of oocytes in GV stage and metaphase II were assayed by quantitative RT-PCR (means ± standard deviations; n = 3).

Downloaded from jcb.rupress.org on November 18, 2013

Published September 23, 2013

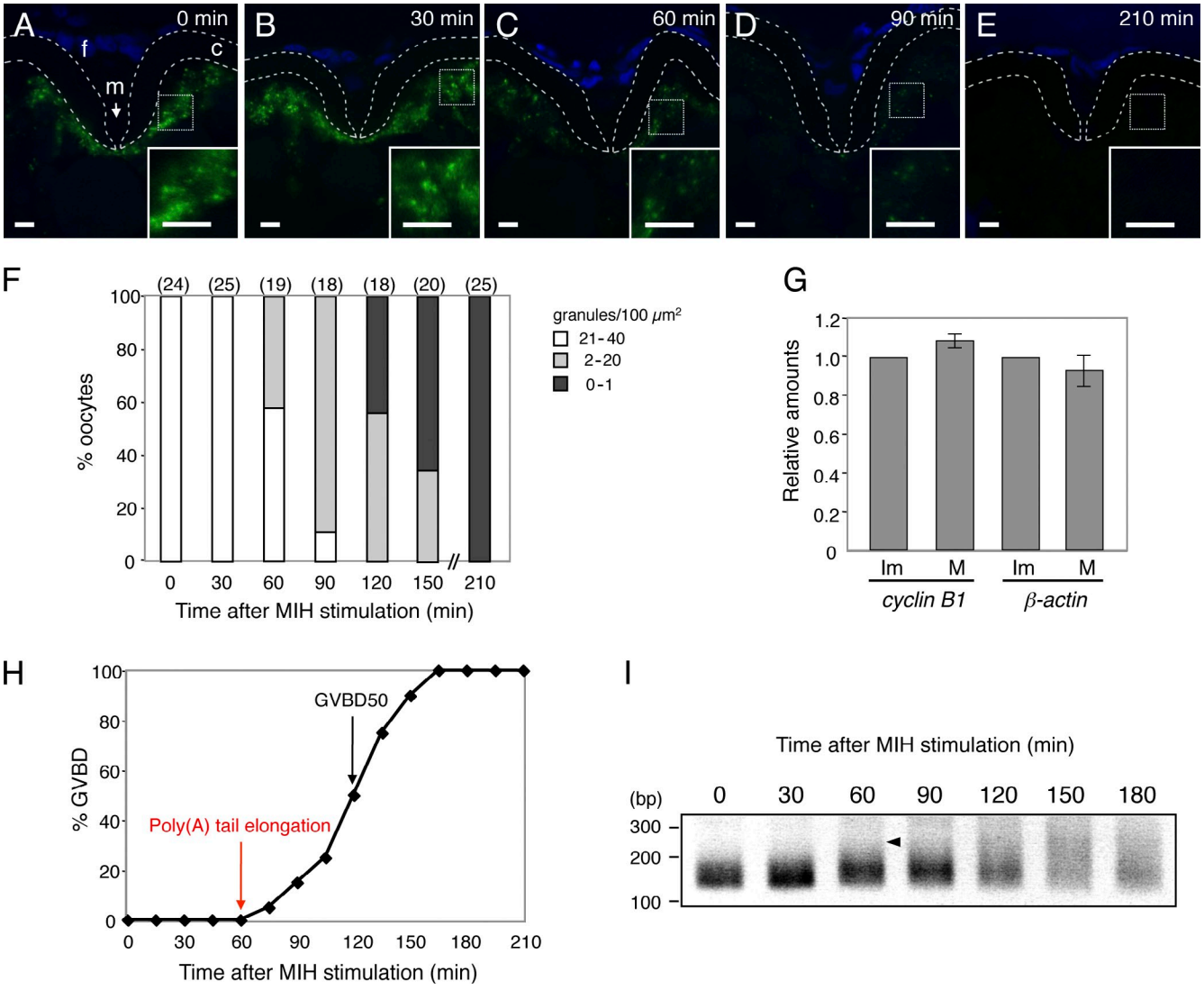


Figure 3. **Zebrafish *cyclin B1* RNA granules disassemble during oocyte maturation.** (A–E) FISH analysis of *cyclin B1* mRNA (green) in zebrafish oocytes at 0 (A), 30 (B), 60 (C), 90 (D), and 210 min (E) after induction of oocyte maturation. DNA is shown in blue. Insets are enlarged views of the boxed regions. Chorions are outlined by broken lines. f, follicle cells; m, micropile; c, chorion. Bars, 5 µm. (F) The number of RNA granules per 100 µm^2 in individual oocytes was counted and categorized as indicated. The numbers in parentheses indicate the total number of oocytes analyzed. Similar results were obtained from two independent experiments. (G) *cyclin B1* and *β-actin* mRNAs from equal numbers of immature (Im) and mature (M) oocytes were assayed by quantitative RT-PCR (means ± standard deviations; $n = 4$). (H) Time course of GVBD after MIH stimulation. (I) Time course of PAT assay for *cyclin B1* mRNA after MIH stimulation. An arrowhead indicates an initial signal of poly(A) tail elongation.

degradation. In contrast, *α-tubulin* mRNA remained uniformly distributed during maturation (Fig. S2).

Oocyte maturation in zebrafish was induced in vitro by stimulation with 17α,20β-dihydroxy-4-pregnen-3-one, a maturation-inducing hormone (MIH) in fish. Dense *cyclin B1* RNA granules (21–40/100 µm^2) were detected in oocytes at 0–30 min after MIH stimulation (Fig. 3, A, B, and F). A decrease in the number of granules (2–20/100 µm^2) began at 60 min after MIH stimulation (Fig. 3, C, D, and F), at which time no oocytes had undergone GVBD (Fig. 3 H). Disappearance of granules (~1/100 µm^2) was observed in oocytes 120 min after MIH stimulation (Fig. 3, E and F). The amount of *cyclin B1* mRNA was not reduced in matured oocytes (Fig. 3 G), indicating that the decrease in number of granules is caused by granule disassembly. The timing when granules began to disassemble (60 min) was correlated with the timing of poly(A) tail elongation of *cyclin B1* mRNA as detected by poly(A) test (PAT) assay (Fig. 3 I). These results suggest a link between granule disassembly and translational activation of *cyclin B1* mRNA after induction of maturation.

Timing of granule disassembly and translational activation of *cyclin B1* mRNA

To clarify the link between granule disassembly and translational activation of *cyclin B1* mRNA more precisely, we used transgenic zebrafish, in which the translational activation of *cyclin B1* mRNA can be visualized in real time with reporter mRNA transcribed in oocytes (Yasuda et al., 2010). The reporter mRNA consists of the full-length *cyclin B1* and the sequence encoding the tetracysteine (TC) tag and GFP, which is inserted downstream of the *cyclin B1* 5′UTR (Fig. 4 A; see also Fig. 6 C).

Downloaded from jcb.rupress.org on November 18, 2013

Published September 23, 2013

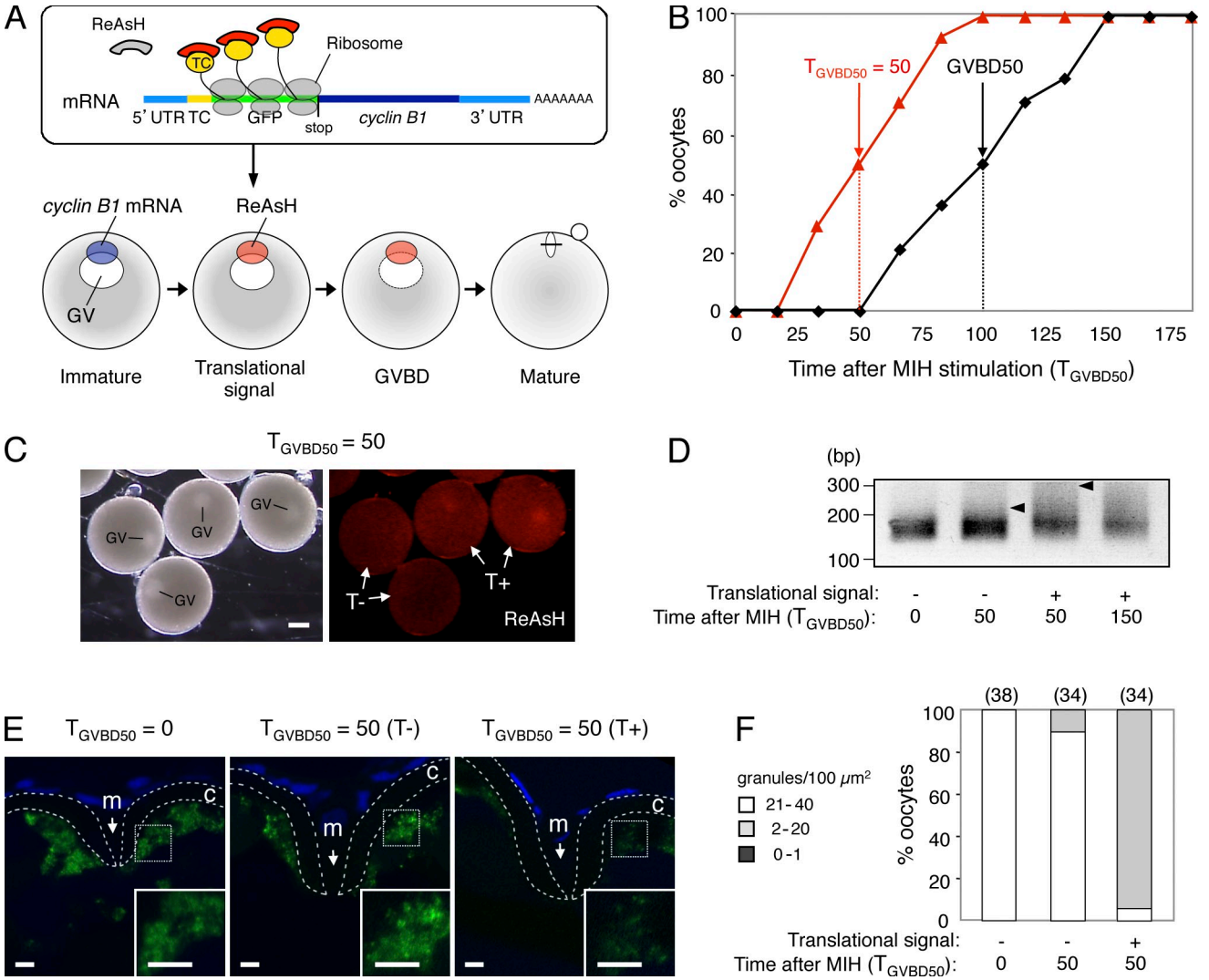


Figure 4. **Timing of *cyclin B1* RNA granule disassembly coincides with that of translational activation.** (A) Schematic views for visualization of site and timing of translation during oocyte maturation. (top) The *cyclin B1* reporter mRNA carries sequences encoding the TC tag (TC) and GFP downstream of *cyclin B1* 5′UTR. The biarsenical dye ReAsH emits no fluorescence in the absence of interaction with the TC tag. Translational activation of the reporter mRNA is visualized by binding of ReAsH to the nascent TC tag peptide, which immediately emits fluorescence. (bottom) The *cyclin B1* reporter mRNA localized at the animal polar cytoplasm of an immature oocyte shows a translational signal at approximately half of the time point at which GVBD occurred. (B) Time course of translational signals (red triangles) and GVBD (black squares). (C) Translational signals at the time T_{GVBD50} = 50. Half of the oocytes show a translational signal (T+), whereas the remaining oocytes show no translational signal (T−). GV, germinal vesicle. Bar, 200 µm. (D) PAT assay of *cyclin B1* mRNA at the time T_{GVBD50} = 0, 50, and 150 of the oocytes exhibiting no translational signal (−) or the oocytes exhibiting a translational signal (+). Arrowheads indicate poly(A) tails at the time T_{GVBD50} = 50. (E) FISH analysis of *cyclin B1* mRNA (green) at the time T_{GVBD50} = 0 and 50 of the oocytes exhibiting no translational signal (T−) or the oocytes exhibiting a translational signal (T+). DNA is shown in blue. Insets are enlarged views of the boxed regions. Chorions are outlined by broken lines. m, micropile; c, chorion. Bars, 5 µm. (F) The number of RNA granules per 100 µm^2 in individual oocytes was counted and categorized as indicated. The numbers in parentheses indicate the total number of oocytes analyzed. Similar results were obtained from three independent experiments.

Translational activation of the reporter mRNA is visualized by binding of a biarsenical dye, ReAsH, to a nascent TC tag, which immediately emits fluorescence (Fig. 4 A).

First, we visualized translational activation of the reporter mRNA in a pool of 20–30 oocytes. As reported previously (Yasuda et al., 2010), translational signals of the reporter mRNA were detected at half of the time point when oocytes underwent GVBD in individual oocytes; therefore, the time when 50% of oocytes exhibited translational signal was half of the time when 50% of the oocytes underwent GVBD (Fig. 4 B). Because oocytes derived from different females underwent GVBD at different times after MIH stimulation (from 90 to 150 min), we expressed the time when 50% of the oocytes underwent GVBD as T_{GVBD50} = 100 (Fig. 4 B). We then separated the oocytes at the time T_{GVBD50} = 50 (Fig. 4 C) according to the presence or absence of the signal and examined them by PAT assay and FISH analysis. Poly(A) tails of c*yclin B1* mRNA remained short in oocytes exhibiting no translational signal (Fig. 4 D, T−), whereas the poly(A) tail was elongated in oocytes exhibiting a translational signal (Fig. 4 D, T+). The dense *cyclin B1* RNA granules were maintained in oocytes exhibiting no translational signal (Fig. 4, E and F, T−) as in those fixed immediately after MIH

Downloaded from jcb.rupress.org on November 18, 2013

Published September 23, 2013

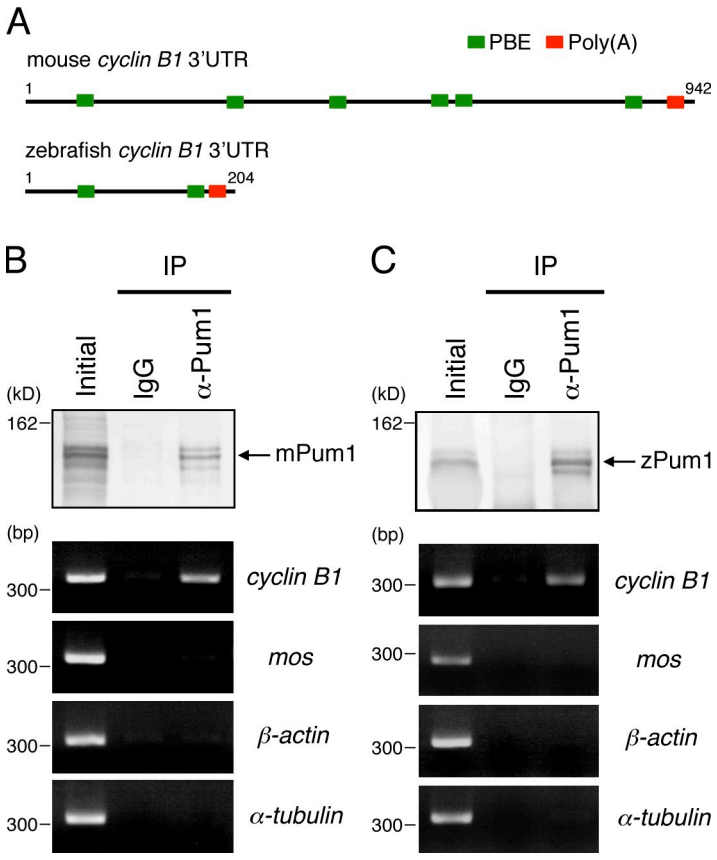


Figure 5. **Mouse and zebrafish Pum1 proteins associate with *cyclin B1* mRNAs.** (A) Schematic diagrams of mouse and zebrafish *cyclin B1* 3′UTRs. Green rectangles indicate putative PBEs, and red rectangles indicate the poly(A) signal. (B, top) Immunoblotting of mouse ovary extracts before IP (Initial) and IP with goat IgG (IgG) or anti-Pum1 goat antibody (α-Pum1). (bottom) RT-PCR amplification for *cyclin B1*, *mos*, *β-actin*, and *α-tubulin* transcripts. (C, top) Immunoblotting of zebrafish ovary extracts before IP (Initial) and IP with rabbit IgG (IgG) or anti-Pum1 rabbit antibody (α-Pum1). (bottom) RT-PCR amplification for *cyclin B1*, *mos*, *β-actin*, and *α-tubulin* transcripts. Similar results were obtained from three independent experiments.

stimulation, whereas the number of RNA granules was decreased in oocytes exhibiting a translational signal (Fig. 4, E and F, T+). Therefore, the timing of *cyclin B1* RNA granule disassembly coincides with the timing of translational activation.

Pum1-mediated RNA granule formation

To assess the function of RNA granules in translational control, we then analyzed molecular mechanisms of *cyclin B1* RNA granule formation. Biochemical analyses in *Xenopus* oocytes have demonstrated that Pum1 regulates the timing of translational activation of *cyclin B1* mRNA (Nakahata et al., 2003; Ota et al., 2011). However, involvement of Pum1 in translational control of *cyclin B1* mRNA in mouse and zebrafish was not shown. Because *Drosophila* Pumilio has the ability to assemble into foci (Salazar et al., 2010), Pum1 was predicted to play a key role in RNA granule formation. To assess this possibility, we first analyzed whether Pum1 binds to *cyclin B1* mRNA in mouse and zebrafish oocytes.

We defined a sequence UGUA as putative PBE, which is part of the Pumilio target consensus sequence UGUANAUA (in which N is any nucleotide), and found that mouse *cyclin B1* mRNA contains several putative PBEs in its 3′UTR (Fig. 5 A). Although no PBE was detected in a recent study (Zhang and Sheets, 2009), we found two putative PBEs in zebrafish *cyclin B1* 3′UTR because of differences in the sequence of PBE and the length of 3′UTR referred in this study (Fig. 5 A). To determine whether Pum1 associates with *cyclin B1* mRNA in mouse and zebrafish oocytes, we first performed an immunofluorescence analysis with anti-Pum1 antibodies, but no signal was detected in either mouse or zebrafish oocytes. The association of *cyclin B1* mRNA with Pum1 was then examined by immunoprecipitation (IP) of mouse and zebrafish ovaries with anti-Pum1 antibodies followed by RT-PCR (IP/RT-PCR). This assay would detect their association in oocytes because follicle cells do not express *pum1* transcripts in both mouse and zebrafish (Fig. S3, A–D). The *cyclin B1* mRNA was detected in precipitations with anti-Pum1 antibodies but not in those with control IgG in both mouse and zebrafish ovaries (Fig. 5, B and C). In contrast, neither *mos*, *β-actin*, nor *α-tubulin* mRNA was detected in precipitations with anti-Pum1 antibodies, indicating the specificity of Pum1 targets. Similar results were obtained using isolated mouse oocytes (Fig. S3 E). Collectively, the results indicate that Pum1 binds to *cyclin B1* mRNA in both mouse and zebrafish oocytes.

To investigate the roles of Pum1 in *cyclin B1* mRNA regulation, we generated transgenic zebrafish expressing a mutant *cyclin B1* reporter mRNA that is incapable of binding to Pum1. We first determined the Pum1 binding site of zebrafish *cyclin B1* mRNA by a UV cross-linking assay. A wild-type (WT) RNA probe containing the *cyclin B1* ORF and 3′UTR and mutant probes carrying mutations in the PBE1 site (PBE1^{m}) or PBE2 site (PBE2^{m}; Fig. 6 A) were incubated with Pum1. As a control, a β-globin probe was also included. The WT and PBE2^{m} probes were associated with Pum1, whereas the PBE1^{m} and control β-globin probes were not (Fig. 6 B), suggesting that the PBE1 sequence is responsible for Pum1 binding. We then generated transgenic fish carrying the *cyclin B1*-PBE1^{m} reporter gene

Downloaded from jcb.rupress.org on November 18, 2013

Published September 23, 2013

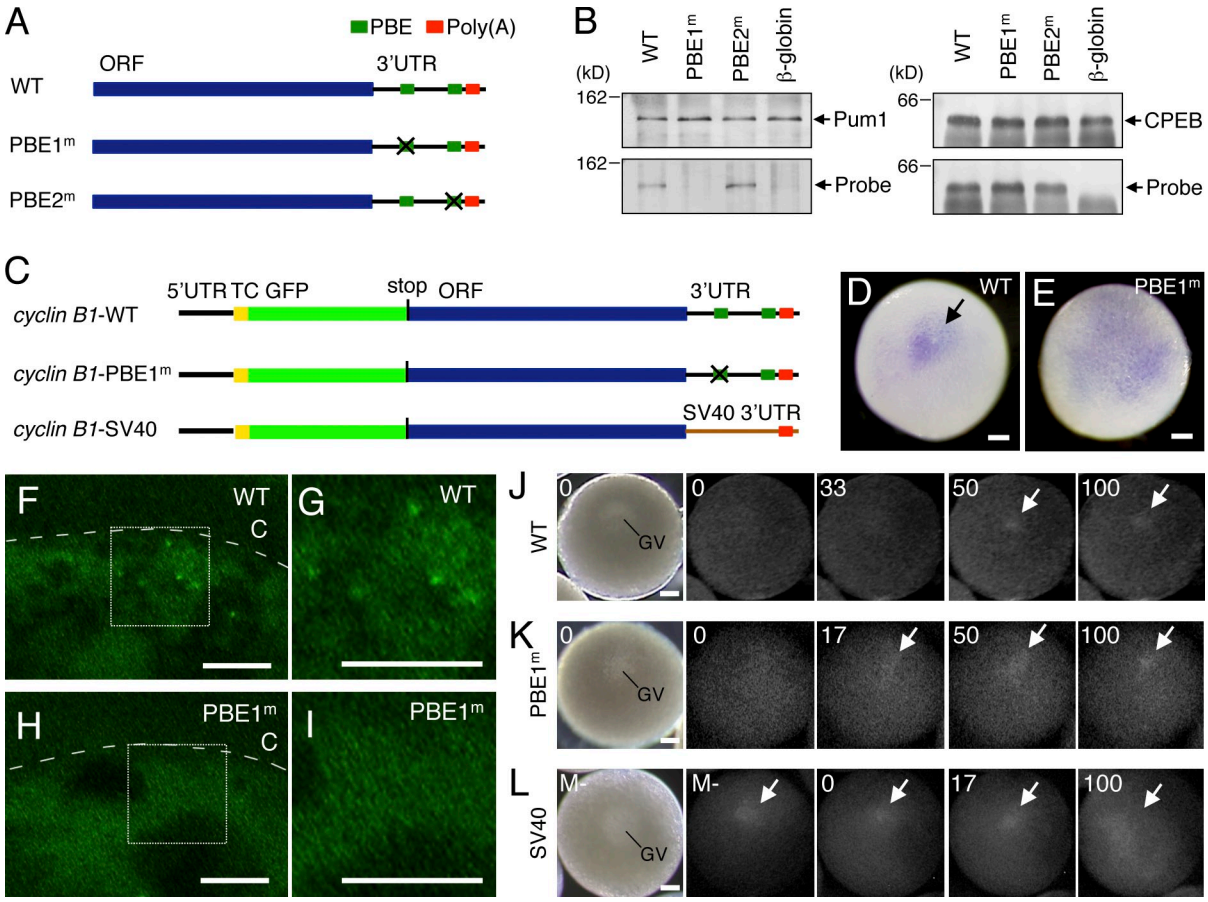


Figure 6. **Binding of *cyclin B1* mRNA to Pum1 is required for granule formation and regulation of accurate timing of translational activation.** (A) Schematic diagrams of RNA probes used for UV cross-linking assay. The WT probe consists of *cyclin B1* ORF and 3′UTR. The PBE1^{m} probe carries mutation in PBE at nucleotides 1,338–1,350 of *cyclin B1* cDNA. The PBE2^{m} probe carries mutation in PBE at nucleotides 1,465–1,468. (B) UV cross-linking assay of *cyclin B1* probes with Pum1 (left) and CPEB (right). (C) Schematic diagrams of reporter mRNAs used for production of transgenic fish. (D and E) Whole-mount in situ hybridization of *cyclin B1*-WT (D) and *cyclin B1*-PBE1^{m} (E) mRNAs. (F–I) FISH analysis of *cyclin B1*-WT (F and G) and *cyclin B1*-PBE1^{m} (H and I) mRNAs. Oocytes are outlined by broken lines. c, chorion. G and I are enlarged views of the boxed regions in F and H. (J–L) Real-time images of translational activation of *cyclin B1*-WT (J), -PBE1^{m} (K), and -SV40 (L) mRNAs. GV, germinal vesicle. Arrows indicate translational signals of the reporter mRNAs. Bars: (D, E, and J–L) 100 µm; (F–I) 5 µm.

(Fig. 6 C) and confirmed interactions of the reporter mRNAs with Pum1 by IP/RT-PCR assay. The *cyclin B1*-WT mRNA was detected in precipitates with the anti-Pum1 antibody, whereas the *cyclin B1*-PBE1^{m} mRNA was not (Fig. S4 A). CPEB was associated with the probes (Fig. 6 B) and reporter mRNAs (Fig. S4 B) irrespective of the mutation in PBE1, indicating that the mutation in PBE1 disrupts binding of Pum1 without affecting that of CPEB.

The localization of *cyclin B1*-PBE1^{m} mRNA in full-grown oocytes was examined by whole-mount in situ hybridization. The *cyclin B1*-WT mRNA was aggregated in the cortical cytoplasm beneath the animal pole of oocytes (100%; n = 37; Fig. 6 D, arrow) as is endogenous *cyclin B1* mRNA (Yasuda et al., 2010), whereas the *cyclin B1*-PBE1^{m} mRNA was distributed throughout the hemisphere of oocytes (100%; n = 118; Fig. 6 E). Although *cyclin B1*-WT mRNA-containing granules were detected by FISH analysis (Fig. 6, F and G), *cyclin B1*-PBE1^{m} mRNA-containing granules were not detected (Fig. 6, H and I). These results indicate that binding of Pum1 is required for the localization of *cyclin B1* mRNA at the animal polar cytoplasm and for the formation of granules.

Precocious translational activation of mutant *cyclin B1* reporter mRNAs

To clarify the role of Pum1 in translational control of *cyclin B1* mRNA, we observed timing of translational activation of the *cyclin B1*-PBE1^{m} mRNA by visualization of the site and timing of translation. As a control, we produced transgenic fish carrying the *cyclin B1*-SV40 reporter gene, in which the *cyclin B1* 3′UTR was substituted with the SV40 3′UTR (Fig. 6 C). This reporter mRNA was neither localized nor assembled into granules (Fig. S4, C and D). The time when individual oocytes underwent GVBD after MIH stimulation was expressed as T_{GVBD} = 100 in this assay. Because the reporter mRNAs contain the stop codon upstream of the *cyclin B1* ORF (Fig. 6 C), their translational products consist of TC-tagged GFP protein but not Cyclin B1 protein and therefore do not affect the progression of oocyte maturation. As reported previously, translational signals of *cyclin B1*-WT mRNA were detected at $T_{GVBD} = 52.9 \pm 4.1$ ($n = 8$; Fig. 6 J; Yasuda et al., 2010). Translational signals of *cyclin B1*-PBE1^{m} mRNA were not detected before MIH stimulation but were observed at $T_{GVBD} = 18.8 \pm 7.5$ ($n = 8$), earlier than translational signals of *cyclin B1*-WT mRNA, after induction of maturation

Downloaded from jcb.rupress.org on November 18, 2013

Published September 23, 2013

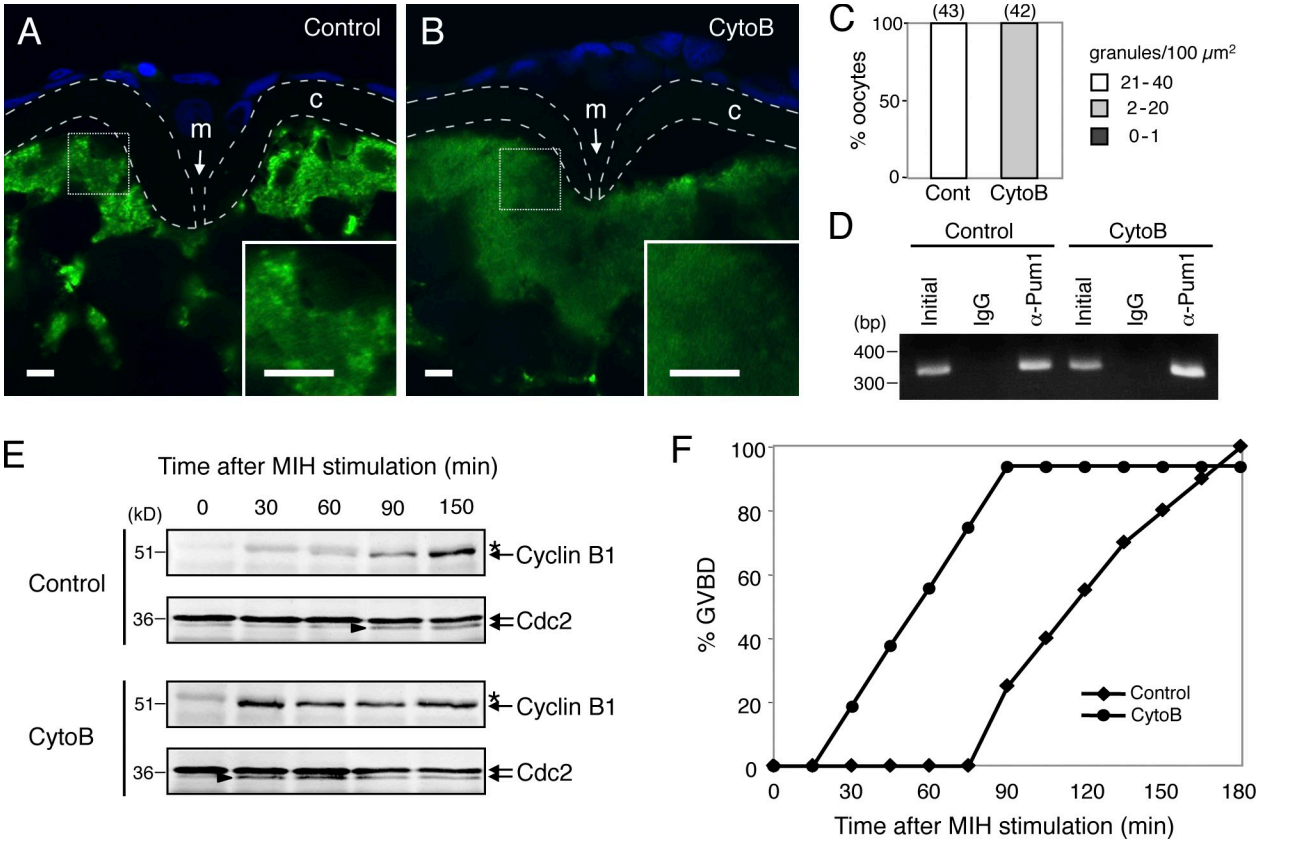


Figure 7. **Depolymerization of actin filaments causes disassembly of *cyclin B1* RNA granules and acceleration of translational activation.** (A and B) FISH analysis of *cyclin B1* mRNA (green) in control (A) and cytochalasin B (CytoB)–treated (B) zebrafish oocytes. DNA is shown in blue. Insets are enlarged views of the boxed regions. Chorions are outlined by broken lines. m, micropile; c, chorion. Bars, 5 µm. (C) The number of RNA granules per 100 µm² in individual oocytes was counted and categorized as indicated. The numbers in parentheses indicate the total number of oocytes analyzed. Similar results were obtained from three independent experiments. (D) RT-PCR amplification for *cyclin B1* of extracts from control (Control) and CytoB-treated oocytes before IP (Initial) and IP with rabbit IgG (IgG) or anti-Pum1 rabbit antibody (α-Pum1). (E) Time course of Cyclin B1 synthesis after induction of oocyte maturation. Arrowheads indicate active forms of the Cdc2 kinase. Asterisks show nonspecific bands. (F) Time course of GVBD after induction of oocyte maturation in the control and CytoB-treated oocytes. Similar results were obtained from three independent experiments.

($P < 0.01$; Fig. 6 K). In contrast, translational signals of *cyclin B1*-SV40 mRNA were detected before MIH stimulation ($n = 8$; Fig. 6 L). Consistent with these results, GFP fluorescence was detectable in oocytes expressing *cyclin B1*-SV40 mRNA during oogenesis, whereas it was undetectable in oocytes expressing *cyclin B1*-WT or -PBE1^{m} mRNA (Fig. S4, E–G). Therefore, binding of Pum1 is not required for translational repression of *cyclin B1* mRNA during oogenesis. Instead, binding of Pum1 to *cyclin B1* mRNA is required for the regulation of accurate timing of translational activation during oocyte maturation.

Effects of actin filament depolymerization on granules and temporal translation of *cyclin B1* mRNA

The anchoring of *cyclin B1* mRNA at the animal polar cytoplasm of zebrafish oocytes depends on actin filaments for the following reasons. (a) Treatment of the oocytes with a lower concentration (1 µg/ml) of cytochalasin B (CytoB), a reagent promoting depolymerization of actin filaments, causes relocation of *cyclin B1* mRNA within the cytoplasm. (b) Treatment with a higher concentration (10 µg/ml) of CytoB disrupts the *cyclin B1* mRNA localization followed by protein synthesis and GVBD, without MIH stimulation. (c) The meshwork of actin filaments disappears during oocyte maturation (Kondo et al., 2001). To further assess the mechanisms of *cyclin B1* RNA granule formation and its role in mRNA regulation, we then analyzed the effects of depolymerization of actin filaments on RNA granules and their translational control.

We treated zebrafish oocytes with a low concentration of CytoB (1 µg/ml) for 3 h because this treatment enables examination of the effects of depolymerization of actin filaments without induction of GVBD. FISH analysis showed that depolymerization of actin filaments caused disassembly of *cyclin B1* RNA granules, such that no granules were detected (Fig. 7, B and C), whereas granules were present in control oocytes (Fig. 7, A and C). Binding of Pum1 to *cyclin B1* mRNA was not affected by depolymerization of actin filaments because semiquantitative IP/RT-PCR assay showed that equivalent amounts of *cyclin B1* mRNA were copurified with the anti-Pum1 antibody in control and CytoB-treated oocytes (Fig. 7 D).

The effect of depolymerization of actin filaments on translational control of *cyclin B1* mRNA was examined by immunoblotting of Cyclin B1 at intervals of 30 min after induction of maturation. As reported previously, Cyclin B1 synthesis was

Downloaded from jcb.rupress.org on November 18, 2013

Published September 23, 2013

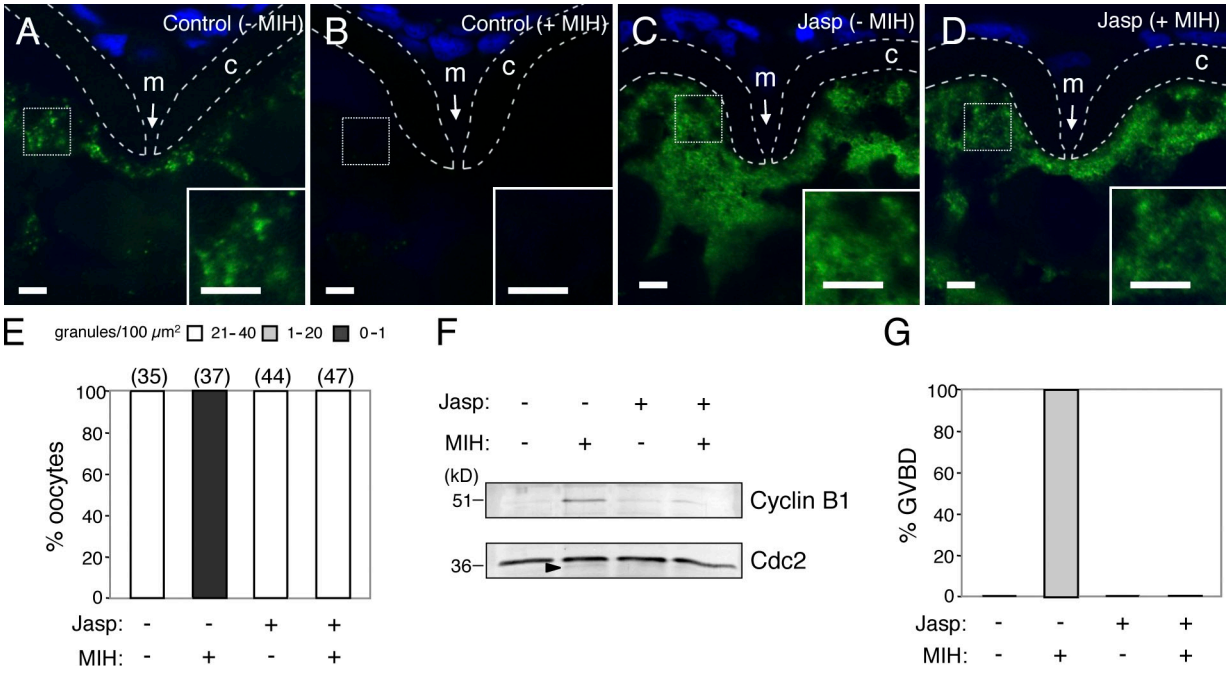


Figure 8. **Stabilization of actin filaments prevents disassembly of *cyclin B1* RNA granules and their translational activation.** (A–D) FISH analysis of *cyclin B1* mRNA (green) in control (A and B) and jasplakinolide (Jasp)-treated oocytes (C and D), stimulated with (B and D) or without (A and C) MIH. DNA is shown in blue. Insets are enlarged views of the boxed regions. Chorions are outlined by broken lines. m, micropile; c, chorion. Bars, 5 µm. (E) The number of RNA granules per 100 µm^2 in individual oocytes was counted and categorized as indicated. The numbers in parentheses indicate the total number of oocytes analyzed. Similar results were obtained from two independent experiments. (F) Immunoblotting of Cyclin B1 and Cdc2 in oocytes stimulated with (+) or without (−) Jasp and MIH. An arrowhead indicates the active form of Cdc2 kinase. (G) Percentage of oocytes stimulated with (+) or without (−) Jasp and MIH that induced GVBD. Similar results were obtained from four independent experiments.

first detected at the time of GVBD (90 min) in control oocytes (Fig. 7, E and F; Kondo et al., 2001). Intriguingly, Cyclin B1 synthesis was not detected in oocytes treated with CytoB for 3 h (0 min) but became detectable (30 min) earlier than in control oocytes (90 min) after induction of maturation (Fig. 7 E). The precocious synthesis of Cyclin B1 directly correlated with the precocious onset of GVBD (Fig. 7 F). These results clearly indicate that formation of microscopically visible RNA granule is not essential for the translational repression of *cyclin B1* mRNA in immature oocytes. RNA granule formation, rather, seems to be necessary for maintaining their repression state until the time when translational products are needed, in this case, for induction of GVBD at the accurate timing in response to MIH stimulation, which is important for proper spindle formation (Kotani and Yamashita, 2002). Our results also indicate that binding of Pum1 is not sufficient for the translational control of *cyclin B1* mRNA.

Effects of actin filament stabilization on granules and translation of *cyclin B1* mRNA

We then examined the effects of stabilization of actin filaments on *cyclin B1* RNA granules and their translational control. Zebrafish oocytes were treated with jasplakinolide (Jasp), a reagent promoting stabilization of actin filaments, for 3 h. Half of the oocytes were then treated with MIH. The actin filaments were depolymerized in the control oocytes in response to MIH, whereas Jasp treatment prevented depolymerization of actin filaments in the oocytes stimulated with MIH (Fig. S5, A–D). FISH analysis showed that *cyclin B1* RNA granules almost completely disappeared in the control mature oocytes (Fig. 8, B and E), whereas those in the oocytes stimulated with Jasp and MIH were maintained (Fig. 8, D and E). Cyclin B1 synthesis was detected in control mature oocytes but was not observed in oocytes stimulated with Jasp and MIH (Fig. 8 F), and these oocytes failed to undergo GVBD (Fig. 8 G). Disassembly of *cyclin B1* RNA granules and GVBD were caused by further treatment of the oocytes with a high concentration of CytoB (10 µg/ml; Fig. S5, E–G), indicating that the stabilization of actin filaments was the cause of impairments of RNA granule disassembly and GVBD in the oocytes stimulated with MIH. These results suggest that *cyclin B1* RNA granule disassembly, which depends on depolymerization of actin filaments, is necessary for translational activation of the mRNA.

Effects of overexpression of Pum1 N terminus on granules and translation of *cyclin B1* mRNA

A recent study has shown that Pumilio proteins contain glutamine/asparagine (Q/N)-rich domains at their N-terminal regions, which promote ordered aggregation of the proteins (Salazar et al., 2010). Therefore, it was expected that overexpression of this region would stabilize RNA granules by assembling into ordered aggregations and sequestering RNA. To analyze effects of RNA granule stabilization on translational control more directly, we expressed GFP-Pum1N containing the Q/N-rich domain (371–494 amino acids) but lacking the C-terminal Puf domain, a

Downloaded from jcb.rupress.org on November 18, 2013

Published September 23, 2013

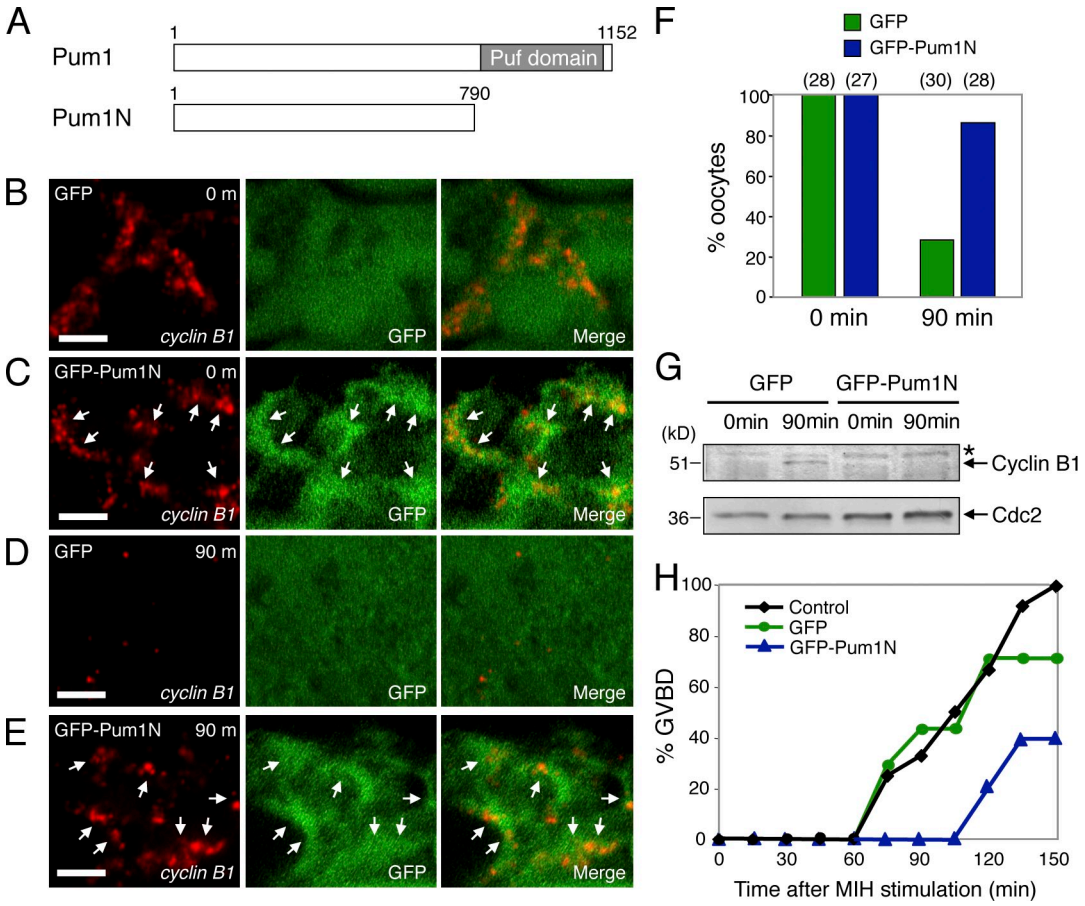


Figure 9. **N terminus of Pum1 stabilizes *cyclin B1* RNA granules and hinders their translational activation.** (A) Schematic diagrams of zebrafish Pum1 and Pum1N. The Puf domain is responsible for binding to PBE in target mRNAs. (B–E) FISH analysis of *cyclin B1* mRNA (red) and immunostaining of GFP (green) in oocytes expressing GFP (B and D) or GFP-Pum1N (C and E) before (B and C) or at 90 min after induction of oocyte maturation (D and E). Merged images are shown (Merge). Arrows indicate aggregation of GFP-Pum1N surrounding cyclin B1 RNA granules. Bars, 5 µm. (F) The number of RNA granules per 100 µm^2 in individual oocytes was counted and categorized. Percentage of oocytes categorized as dense (21–40) is shown. The numbers in parentheses indicate the total number of oocytes analyzed. Similar results were obtained from three independent experiments. (G) Immunoblotting of Cyclin B1 and Cdc2 in oocytes expressing GFP and GFP-Pum1N before (0 min) and at 90 min after induction of oocyte maturation. An asterisk shows a nonspecific band. The active form of Cdc2 kinase was undetectable in the oocytes at these time points. (H) Time course of GVBD after induction of oocyte maturation in the control, GFP-expressing, and GFP-Pum1N–expressing oocytes. Similar results were obtained from three independent experiments.

region required for binding to PBE (Fig. 9 A; Zamore et al., 1997; Zhang et al., 1997), in zebrafish oocytes by injection of mRNA. Aggregation of GFP-Pum1N surrounding *cyclin B1* RNA granules was detected (Fig. 9 C, arrows), whereas in controls, GFP was distributed throughout the cytoplasm (Fig. 9 B). We then examined the effect of overexpressing GFP-Pum1N during oocyte maturation. *cyclin B1* RNA granules were disassembled at 90 min after induction of maturation in control oocytes expressing GFP (Fig. 9, D and F) as was the case for uninjected oocytes (Fig. 3, D and F), whereas the granules were maintained in oocytes expressing GFP-Pum1N (Fig. 9, E and F). Cyclin B1 protein was detectable at 90 min after induction of maturation in control oocytes, whereas Cyclin B1 remained undetectable in oocytes expressing GFP-Pum1N (Fig. 9 G). Although GVBD was not completely prevented, the timing of GVBD after induction of maturation was significantly delayed in oocytes expressing GFP-Pum1N (Fig. 9 H). These results strongly suggest that translational activation of *cyclin B1* mRNA requires disassembly of RNA granules.

Discussion

RNA granules in vertebrate oocytes

RNA granule formation within oocytes has been identified in invertebrates, *Drosophila* and *C. elegans* (Mahowald, 1971; Seydoux and Fire, 1994; Kato and Nakamura, 2012). Furthermore, recent studies have demonstrated the existence of several classes of RNA granules and the identification of hundreds of assembled RNAs in *C. elegans* oocytes (Boag et al., 2008; Noble et al., 2008). In contrast to invertebrates, only the *Xenopus* germinal granule was shown to contain mRNAs in vertebrate oocytes (Kloc et al., 2002). *Xenopus* germinal granules are located at the vegetal polar cytoplasm of the oocyte beneath the mitochondrial cloud (also known as Balbiani body) and assemble mRNAs encoding Xcat2, Xpat, and DEADSouth, which are thought to play important roles in germ cell development after fertilization. In this study, we detected *cyclin B1* mRNA in granules in the animal polar cytoplasm of zebrafish oocytes and in the cytoplasm of mouse oocytes (Fig. 1), which might be

Downloaded from jcb.rupress.org on November 18, 2013

Published September 23, 2013

distinct from germinal granules in *Xenopus* because the Balbiani body and germ plasm components, such as *DAZ-like* mRNA, are also located in the vegetal polar cytoplasm of zebrafish oocytes (Kosaka et al., 2007). In this regard, it is notable that *Xenopus cyclin B1* mRNA is also localized at the animal pole of embryos (Groisman et al., 2000). A recent study has shown that full-grown mouse oocytes contain subcortical aggregates (SCAs) of several P-body components (Flemr et al., 2010). *cyclin B1* RNA granules might be distinct from SCAs because (a) *cyclin B1* RNA granules are mainly distributed in the cytoplasm (Fig. 1 and Fig. 2), whereas SCAs are accumulated in the subcortical region, and (b) *cyclin B1* mRNA-containing granules are compositionally related to SGs (Fig. S1), whereas SCAs are related to P bodies.

An intriguing finding in this study is that full-grown mouse oocytes exhibited molecular asymmetry, i.e., asymmetrical distribution of *cyclin B1* RNA granules within the cytoplasm (Fig. 1 and Fig. 2). It has been widely believed that mouse oocytes are symmetrical and nonpolar. However, recent studies have shown the existence of a Balbiani body (Pepling et al., 2007) and cytoplasmic polarity (Kloc et al., 2008) in the early developmental stages of mouse oocytes, suggesting a conserved process of early oocyte development in vertebrates. Although whether the polarity observed in full-grown mouse oocytes is similar to that found in *Xenopus* and zebrafish oocytes remains to be elucidated, our finding that *cyclin B1* mRNA is localized as granules in full-grown mouse and zebrafish oocytes suggests that the cellular and molecular mechanisms of oocyte development in vertebrates are conserved.

Translational control of *cyclin B1* mRNA through formation and disassembly of RNA granules

The biochemical details of translational control of *cyclin B1* mRNA have been extensively studied in *Xenopus* oocytes (Mendez and Richter, 2001; de Moor et al., 2005). The main cis-acting element that regulates translational repression and activation of *Xenopus cyclin B1* mRNA is the CPE located in the 3′UTR, and its binding protein, CPEB, functions as the trans-acting factor. Maskin binds to both the CPEB and the cap-binding protein eIF4E, preventing recruitment of eIF4G and the 40S ribosomal subunit to eIF4E. After induction of oocyte maturation, CPEB recruits cleavage and polyadenylation specificity factor to the poly(A) signal. Cleavage and polyadenylation specificity factor brings the poly(A) polymerase to the mRNA. Elongation of the poly(A) tail by poly(A) polymerase recruits poly(A)-binding protein, which promotes dissociation of Maskin from eIF4E, resulting in recruitment of eIF4G and the 40S ribosomal subunit to eIF4E and subsequent translational activation of the mRNA. Pum1 is a member of the Puf family of RNA-binding proteins that is highly conserved from yeast to mammals. Pum1 binds to both the *Xenopus cyclin B1* mRNA and CPEB (Nakahata et al., 2001; Piqué et al., 2008) and plays a role in determining the timing of *cyclin B1* translational activation (Nakahata et al., 2003; Ota et al., 2011). However, the molecular and cellular mechanisms of translational control of *cyclin B1* mRNA and the precise function of Pum1 in temporal control of translation have not been elucidated.

In this study, we report for the first time that translationally repressed *cyclin B1* mRNAs form granules in oocytes. Pum1 also binds to the mouse and zebrafish *cyclin B1* mRNAs in oocytes (Fig. 5). Recent studies have shown that the Q/N-rich domain of *Drosophila* Pumilio has the ability to assemble into foci when expressed in yeast (Salazar et al., 2010) and that of mammalian Pumilio2 has the ability to form granules in HeLa cells (Vessey et al., 2006). Our results showed that the association of Pum1 at the PBE of *cyclin B1* mRNA is required for granule formation of the mRNA in oocytes (Fig. 6). Therefore, it is likely that Pum1 assembles the *cyclin B1* mRNA into granules via the Q/N-rich domain in oocytes. Alternatively, it is possible that binding of Pum1 modulates the *cyclin B1* mRNA structure and promotes association of other proteins required for granule formation.

Intriguingly, the *cyclin B1* RNA granules were disassembled during oocyte maturation at the time of their poly(A) tail elongation in both the mouse (Fig. 2; Tay et al., 2000) and zebrafish (Fig. 3). Visualization of the site and timing of translation revealed that RNA granule disassembly occurs at the time of translational activation (Fig. 4). Because the mutant *cyclin B1* reporter mRNA that is incapable of binding to Pum1 was still translationally repressed despite the inability to form granules (Fig. 6 and Fig. S4 F), Pum1-mediated granule formation is not essential for the translational repression of target mRNA. Rather, granule formation seems necessary for regulating the time of *cyclin B1* translational activation during oocyte maturation (Fig. 6). Translational repression and activation of *cyclin B1* mRNA might be mainly driven by CPEB, which still binds to the mutant *cyclin B1* reporter mRNA (Fig. 6 B and Fig. S4 B) because mutations in CPEs of *Xenopus cyclin B1* 3′UTR result in derepression of translation in immature oocytes and failure of polyadenylation and translational activation after induction of maturation (de Moor and Richter, 1999). Therefore, Pum1 might function to assemble *cyclin B1* RNA granules, ensuring the timing of translational activation of the target mRNA during oocyte maturation.

We also showed a link between *cyclin B1* RNA granules and actin filaments in zebrafish oocytes (Fig. 7 and Fig. 8). Interestingly, the disassembly of endogenous *cyclin B1* RNA granules by depolymerization of actin filaments did not alter their translational repression states but accelerated the timing of translational activation after induction of maturation (Fig. 7). Therefore, visible granule formation of endogenous *cyclin B1* mRNA is not essential for translational repression but rather is required for the mRNA to be translationally repressed until the protein product is required. In support of this proposal, stabilization of actin filaments prevents the disassembly of granules and translational activation of *cyclin B1* mRNA (Fig. 8).

The significance of RNA granule formation in translational control is further supported by the results of overexpression of Pum1 N terminus, which stabilized *cyclin B1* RNA granules and prevented their translational activation after induction of oocyte maturation (Fig. 9). Although the detailed mechanism by which GFP-Pum1N is aggregated as a form surrounding *cyclin B1* RNA granules remains to be elucidated, direct binding of Pum1N to the mRNA would not be involved because of the lack of C-terminal RNA-binding region, Puf domain (Zamore et al., 1997;

Downloaded from jcb.rupress.org on November 18, 2013

Published September 23, 2013

Zhang et al., 1997). Conversely, despite binding of Pum1 to *cyclin B1* mRNA, the timing of translational activation was accelerated when the granules were disassembled by treatment with CytoB (Fig. 7). Collectively, three independent lines of evidence—one provided by genetic analysis (Fig. 6) and the others by using pharmacological regents (Fig. 7 and Fig. 8) and overexpression of the Pum1 N terminus (Fig. 9)—support the notion that the precise timing of translational activation of *cyclin B1* mRNA is regulated through formation and disassembly of RNA granules during oocyte maturation.

Role of RNA granules in translational control

RNA granules are found in various cell types and organisms and thought to play important roles in mRNA regulation. However, it has been suggested that formation of RNA granules is a consequence of translational repression (Decker et al., 2007; Eulalio et al., 2007). Our results demonstrate that RNA granule formation itself is not essential for translational repression of *cyclin B1* mRNA. However, based on our results in oocyte maturation, we propose a novel function of RNA granules in temporal control of translation; they play a key role in the regulation of accurate timing of translational activation that occurs in response to a specific signal. How then does the *cyclin B1* RNA granule maintain its repression state until the time when their protein products are needed? In this regard, it is notable that *Drosophila oskar* mRNA is assembled into high-order particles, which have been proposed to be inaccessible to translational machinery and thereby effectively repressing mRNA translation (Chekulaeva et al., 2006). The *cyclin B1* RNA granules may be functionally related to the *oskar* RNA particles and be inaccessible to translational machinery. By dissociating from granules, *cyclin B1* mRNAs may become accessible to translational machinery such as the 40S ribosomal subunit. This mechanism would effectively and strictly coordinate the timing of translational activation in temporal control of mRNA translation. Our next goal is to elucidate the molecular mechanism by which dissociation of *cyclin B1* RNA granules is triggered. In addition, further studies on the composition, architecture, and dynamics of *cyclin B1* RNA granules and their sequential changes during oocyte maturation, particularly at the time of granule disassembly, would help in understanding the molecular nature of granule-mediated translational control, which plays crucial roles in cellular, neuronal, and developmental processes in a wide range of organisms from yeast to mammals.

Materials and methods

Preparation of ovaries

All animal experiments in this study were approved by the Committee on Animal Experimentation, Hokkaido University. Zebrafish ovaries were dissected from adult females in zebrafish Ringer's solution (116 mM NaCl, 2.9 mM KCl, 1.8 mM $CaCl_2$, and 5 mM Hepes, pH 7.2). Mouse ovaries were dissected from 8-wk-old C57BL/6J females in PBS (137 mM NaCl, 2.7 mM KCl, 10 mM Na_2HPO_4, and 2 mM KH_2PO_4, pH 7.2). For in situ hybridization analysis, zebrafish and mouse ovaries were fixed with 4% PFA in PBS (4% PFA/PBS) overnight at 4°C. To avoid artifacts in fixation, mouse ovaries were dissected into small pieces (100–200 µm in diameter) with a razor blade under a dissecting microscope and fixed with 4% PFA/PBS overnight at 4°C. For IP/RT-PCR analysis, zebrafish ovaries were homogenized with an equal volume of ice-cold extraction buffer (EB; 100 mM β-glycerophosphate, 20 mM Hepes, 15 mM $MgCl_2$, 5 mM EGTA, 1 mM dithiothreitol, 100 µM (*p*-amidinophenyl)methanesulfonyl fluoride, and 3 µg/ml leupeptin, pH 7.5) containing 100 U/ml RNasin Plus RNase Inhibitor (Promega), and mouse ovaries were homogenized with an equal volume of ice-cold EB containing 1% Tween 20 and 100 U/ml RNasin Plus RNase Inhibitor. After centrifugation at 15,000 *g* for 10 min at 4°C, the supernatant was collected and used for IP. To confirm the interaction of Pum1 with *cyclin B1* mRNA in oocytes, mouse oocytes were retrieved from ovaries in MEM-α by puncturing the ovaries with a needle. 10 µM milrinone was used for preventing resumption of oocyte maturation. 400 immature oocytes (GV stage) were extracted with 200 µl of ice-cold EB containing 1% Tween 20 and 100 U/ml RNasin Plus RNase Inhibitor. After centrifugation at 15,000 *g* for 10 min at 4°C, the supernatant was collected and used for IP.

Section and whole-mount in situ hybridization

Section in situ hybridization was performed according to the procedure reported previously (Kondo et al., 2001). In situ hybridization with the TSA Plus DNP system (PerkinElmer) was performed according to the manufacturer's instructions. In brief, fixed ovaries and oocytes were dehydrated, embedded in paraffin, and cut into 12-µm-thick sections. The digoxigenin (DIG)-labeled antisense RNA probe for full-length *cyclin B1* or ORF of GFP was used for detection of endogenous *cyclin B1* or reporter gene transcript, respectively. No signal was detected with sense probes. After hybridization and washing, samples were incubated with anti-DIG–HRP antibody (1:500 dilution; Roche) for 30 min. The reaction with tyramide-DNP followed by that with the anti-DNP–AP antibody and detection of the signal were performed according to the manufacturer's instructions. For FISH analysis, the samples were incubated with the anti-DNP–Alexa Fluor 488 antibody (1:500 dilution; Molecular Probes) for 3 h after reaction with tyramide-DNP. To detect nuclei, the samples were incubated with 10 µg/ml Hoechst 33258 for 10 min. The samples were observed under a confocal microscope (LSM 5 LIVE; Carl Zeiss) at room temperature using a Plan Apochromat 63×/1.4 NA oil differential interference contrast lens and LSM 5 DUO 4.2 software (Carl Zeiss). The number of *cyclin B1* RNA granules was quantified using IMARIS software (Bitplane), which enables detection of granules according to the size (>0.3 µm) and the intensity at the center of granules. Whole-mount in situ hybridization was performed according to the procedure reported previously (Schulte-Merker et al., 1992). In brief, fixed zebrafish oocytes were treated with 100% methanol and stored at −20°C until further treatment. The oocytes were rehydrated and treated with 10 µg/ml Proteinase K in PBS for 1 min at room temperature. After hybridization and washing, the oocytes were incubated with anti-DIG–AP antibody (1:2,000 dilution; Roche), and the signal was detected according to the manufacturer's instructions.

Induction of oocyte maturation

Zebrafish oocytes were manually isolated from ovaries with forceps under a dissecting microscope (SZ-ST; Olympus). Oocyte maturation in this species was induced by treatment with 1 µg/ml 17α,20β-dihydroxy-4-pregnen-3-one, an MIH in fish. For FISH analysis, oocytes were fixed with 4% PFA/PBS at intervals of 30 min after MIH stimulation. For quantification of the amount of *cyclin B1* mRNA, full-grown immature oocytes and oocytes 3 h after MIH stimulation (matured oocytes) were extracted with Isogen (NIPPON GENE), and the total RNAs were used for quantitative RT-PCR. Oocyte maturation in mice was induced by injection of 5 U of hCG 48 h after injection of 5 U of pregnant mare serum gonadotropin into 3-wk-old females. Ovaries and oviducts were fixed with 4% PFA/PBS at 0, 4, and 14 h after hCG injection for FISH analysis of oocytes in GV stage, prometaphase I, and metaphase II, respectively. For quantification of the amount of *cyclin B1* mRNA, ovaries at 0 and 14 h after hCG injection were dissociated in MEM-α containing 1.5 mg/ml collagenase. 10 µM milrinone was used for preventing resumption of oocyte maturation to collect immature oocytes from ovaries at 0 h after hCG injection. Full-grown immature oocytes (GV stage) and matured oocytes (in metaphase II) were extracted with Isogen, and the total RNAs were used for quantitative RT-PCR.

Quantitative RT-PCR

The expression of *cyclin B1* and *β-actin* mRNAs in full-grown immature and matured oocytes was quantified by using a real-time PCR system with SYBR green PCR Master Mix (Applied Biosystems) according to the manufacturer's instructions. Total RNA extracted from 50 full-grown immature or matured oocytes was used for cDNA synthesis using the SuperScript III First Strand Synthesis System (Invitrogen). The *cyclin B1* and *β-actin* transcripts were amplified with the cDNA and primer sets specific to *cyclin B1* and *β-ctin* mRNA (Table S1).

Downloaded from jcb.rupress.org on November 18, 2013

Published September 23, 2013

PAT assay

RNA ligation-coupled RT-PCR was performed according to the procedure reported previously (Yasuda et al., 2010). 2 µg of total RNA extracted from pools of 15 zebrafish oocytes was ligated to 0.4 µg of P1 anchor primer (Table S1) in a 10-µl reaction using T4 RNA ligase (New England Biolabs, Inc.) for 30 min at 37°C. The ligase was inactivated for 5 min at 92°C. Half of the RNA ligation reaction was used in a 25-µl reverse transcription reaction using SuperScript III First Strand Synthesis System with a P1′ primer (Table S1). 5 µl of the cDNA was used for the first PCR with the P1′ primer and a zebrafish-*cyclin B1*-ORF-f2 primer (Table S1) for 15 cycles. 2 µl of the first PCR reaction was used for the second PCR with the P1′ primer and a zebrafish-*cyclin B1*-3′UTR-f2 primer (Table S1) for 25 cycles. The PCR product was resolved on a 2% TAE (Tris-acetate-EDTA) gel.

Visualization of site and timing of translation

To detect translation of reporter mRNAs in oocytes, 1 nl of 0.2-mM ReAsH dye (Invitrogen) in zebrafish Ringer's solution was injected into full-grown oocytes using a microinjector (CellTram vario; Eppendorf). The ReAsH signal was observed under a fluorescence stereomicroscope (M165 FC; Leica) using a filter set of Texas red and photographed by using a cooled charge-coupled device color camera (VB-7010; Keyence) at intervals of 15 min after MIH stimulation. The images were compiled using Photoshop CS5 software (Adobe).

Production of antibodies

We produced new antibodies that effectively precipitate Pum1 as follows. A GST-fused N terminus fragment of *Xenopus* Pum1 (amino acids 1–410) was expressed in *Escherichia coli*, gel-purified, and injected into two rabbits to produce antibodies as described previously (Kotani et al., 2001). To clone full-length zebrafish *pum1*, we first amplified an EST sequence encoding the N terminus fragment of Pum1 by PCR with a primer set of zPum1-f1 and zPum1-r1 (Table S1). Then, we performed rapid amplification of cDNA ends using the 3′RACE System for Rapid Amplification of cDNA Ends (Invitrogen) with a primer designed within the cloned *pum1* (Table S1). The resulting full-length *pum1* (available at GenBank under accession no. AB841266) was cloned into pGEM-T. A GST-fused N terminus fragment of zebrafish Pum1 (amino acids 1–383) was expressed in *E. coli*, electroblotted onto a membrane (Immobilon; EMD Millipore), and used to affinity purify the rabbit antisera.

RT-PCR analysis after IP (IP/RT-PCR)

100 µl zebrafish ovary extracts was incubated with affinity-purified anti–*Xenopus* Pum1 rabbit antibody or control rabbit IgG, and 80 µl mouse ovary or oocyte extracts was incubated with anti–human Pum1 goat antibody (Bethyl Laboratories, Inc.) or control goat IgG for 1 h at 4°C. The extracts were then incubated with protein A–Sepharose beads (GE Healthcare) for 3 h at 4°C and washed five times with EB containing 1% Tween 20. After extraction of mRNAs from the beads with Isogen, RT-PCR was performed using primer sets specific to *cyclin B1*, *mos*, *β-actin*, and *α-tubulin* mRNA (Table S1).

Immunoblotting

The crude extracts from ovaries and the immunoprecipitates of anti-Pum1 antibodies and control IgGs were separated by SDS-PAGE, blotted onto an Immobilon membrane, and probed with anti–*Xenopus* Pum1 monoclonal antibody (Pum2A5; Nakahata et al., 2001) and anti–human Pum1 antibody. The Cyclin B1–Cdc2 complex was detected by immunoblotting Suc1 precipitates from crude zebrafish oocyte extracts with anti-Cdc2 (MC2-21; Tanaka and Yamashita, 1995) and anti–goldfish Cyclin B1 (B112; Katsu et al., 1993) monoclonal antibodies.

UV cross-linking assay

The ORF of zebrafish *pum1* was cloned into pCS2-Flag-N to produce Pum1 fused with Flag tag at the N terminus of Pum1. The ORF of zebrafish *cpeb* (also known as *zorba*; Bally-Cuif et al., 1998) was cloned into pCS2-Flag-N to produce CPEB fused with Flag tag at the N terminus of CPEB. mRNAs encoding the Pum1-Flag and CPEB-Flag were synthesized with an mMESSAGE mMACHINE SP6 kit (Ambion). 4 µg of the mRNAs was translated in rabbit reticulocyte lysate (Promega). Pum1-Flag and CPEB-Flag were purified by IP with anti-Flag monoclonal antibody (M2; Sigma-Aldrich). The ORF and 3′UTR of zebrafish *cyclin B1* was cloned into pGEM-T. Mutations in PBEs of *cyclin B1* mRNA were introduced using a site-directed mutagenesis kit (QuikChange; Agilent Technologies) with primer sets of PBE1^{m}-f1/PBE1^{m}-r1 and PBE2^{m}-f1/PBE2^{m}-r1 (Table S1). Using the corresponding plasmids as templates, WT, PBE1^{m}, and PBE2^{m} DIG-labeled RNA probes were synthesized with a DIG RNA labeling kit (T7; Roche). 2 µg of the probes was incubated with the purified Pum1-Flag or CPEB-Flag for 30 min at room temperature and irradiated in a UV cross-linker (FS-800; Funakoshi) at an energy setting of 860 mJ/cm^2. After treatment with 200 µg/ml Ribonuclease A (Nacalai) for 15 min at 37°C, the immunoprecipitates were collected and used for immunoblotting.

Production of transgenic zebrafish

Using pT2KXIGΔin-TGO3′ (Yasuda et al., 2010) as a template, the *cyclin B1*-PBE1^{m} reporter gene was produced with a QuikChange site-directed mutagenesis kit and the primer set of PBE1^{m}-f1/PBE1^{m}-r1. The *cyclin B1*-SV40 reporter gene was produced by replacing the *cyclin B1* 3′UTR of pT2KXIGΔ in-TGO3′ with SV40 3′UTR. Transgenic zebrafish was produced using *Tol2* transposon-mediated germline transmission (Kotani et al., 2006; Kotani and Kawakami, 2008). Three lines carrying the same reporter gene were produced and analyzed. All lines carrying the same reporter gene gave equivalent results.

CytoB and Jasp treatments

To depolymerize actin filaments, oocytes were treated with 1 µg/ml CytoB (Sigma-Aldrich) for 3 h. After treatment with CytoB for 3 h, the oocytes were stimulated with MIH for induction of oocyte maturation. To stabilize actin filaments, oocytes were treated with 5 µM Jasp (EMD Millipore) for 3 h. CytoB and Jasp were dissolved in DMSO as stocks and diluted in Ringer's solution before use. As a control, oocytes were treated with 0.01% DMSO (for CytoB) or 0.5% DMSO (for Jasp).

Overexpression of Pum1 N terminus and immunostaining

Sequences encoding the N terminus of zebrafish Pum1 (Pum1N; 1–790 amino acids) were cloned into pCS2-GFP-N to produce Pum1N fused with GFP at the N terminus of Pum1. mRNAs encoding the GFP-Pum1N and GFP were synthesized with an mMESSAGE mMACHINE SP6 kit (Life Technologies). 2 ng of the mRNAs was injected into full-grown oocytes using a microinjector (CellTram vario). The oocytes were incubated for 3 h and stimulated with MIH. Before or at 90 min after MIH stimulation, the oocytes were fixed with 4% PFA/PBS for FISH analysis or extracted with ice-cold EB for detection of Cyclin B1. To detect GFP-Pum1N and GFP, the oocytes were immunostained with the anti-GFP mouse antibody (1:200 dilution; Roche) followed by anti–mouse IgG–Alexa Fluor 488 antibody (1:200 dilution; Molecular Probes), after hybridization and washing of the *cyclin B1* RNA probe in FISH analysis. Similarly, HuR protein was detected with the anti-HuR mouse antibody (3A2; 1:50 dilution; Santa Cruz Biotechnology, Inc.). *cyclin B1* mRNA was detected with the anti-DIG–HRP antibody followed by the reaction with tyramide-Cy3 (PerkinElmer).

Online supplemental material

Fig. S1 shows additional data on distribution of *cyclin B1* and *α-tubulin* mRNAs in mouse and zebrafish oocytes and colocalization of HuR with *cyclin B1* RNA granules. Fig. S2 shows uniform distribution of *α-tubulin* mRNA during mouse oocyte maturation. Fig. S3 shows the restricted expression of *pum1* mRNA in oocytes and the interaction of Pum1 protein with *cyclin B1* mRNA in oocytes. Fig. S4 shows that the interactions of reporter mRNA with Pum1 protein in oocytes are disrupted by mutation in PBE1 and that translation of reporter mRNA carrying mutation in PBE1 is repressed during oogenesis. Fig. S5 shows that Jasp treatment stabilizes actin filaments in oocytes stimulated with MIH and that the effects of Jasp treatment on *cyclin B1* RNA granules and GVBD are caused by the stabilization of actin filaments. Online supplemental material is available at http://www.jcb.org/cgi/content/full/jcb.201302139/DC1. Additional data are available in the JCB DataViewer at http://dx.doi.org/10.1083/jcb.201302139.dv.

This work was supported by a Grant-in-Aid for Young Scientists and a Grant-in-Aid for Scientific Research on Priority Areas "The Germline" (23770196 and 23013001 to T. Kotani) and a Grant-in-Aid for Scientific Research (23370027 to M. Yamashita) from the Ministry of Education, Culture, Sports, Science and Technology, Japan.

Submitted: 26 February 2013
Accepted: 15 August 2013

References

Anderson, P., and N. Kedersha. 2009. RNA granules: post-transcriptional and epigenetic modulators of gene expression. *Nat. Rev. Mol. Cell Biol.* 10:430–436. http://dx.doi.org/10.1038/nrm2694

Baez, M.V., L. Luchelli, D. Maschi, M. Habif, M. Pascual, M.G. Thomas, and G.L. Boccaccio. 2011. Smaug1 mRNA-silencing foci respond to NMDA

Downloaded from jcb.rupress.org on November 18, 2013

Published September 23, 2013

and modulate synapse formation. *J. Cell Biol.* 195:1141–1157. http://dx.doi.org/10.1083/jcb.201108159

Bally-Cuif, L., W.J. Schatz, and R.K. Ho. 1998. Characterization of the zebrafish Orb/CPEB-related RNA binding protein and localization of maternal components in the zebrafish oocyte. *Mech. Dev.* 77:31–47. http://dx.doi.org/10.1016/S0925-4773(98)00109-9

Boag, P.R., A. Atalay, S. Robida, V. Reinke, and T.K. Blackwell. 2008. Protection of specific maternal messenger RNAs by the P body protein CGH-1 (Dhh1/RCK) during *Caenorhabditis elegans* oogenesis. *J. Cell Biol.* 182:543–557. http://dx.doi.org/10.1083/jcb.200801183

Chapman, D.L., and D.J. Wolgemuth. 1992. Identification of a mouse B-type cyclin which exhibits developmentally regulated expression in the germ line. *Mol. Reprod. Dev.* 33:259–269. http://dx.doi.org/10.1002/mrd.1080330305

Chekulaeva, M., M.W. Hentze, and A. Ephrussi. 2006. Bruno acts as a dual repressor of oskar translation, promoting mRNA oligomerization and formation of silencing particles. *Cell*. 124:521–533. http://dx.doi.org/10.1016/j.cell.2006.01.031

Cougot, N., S. Babajko, and B. Séraphin. 2004. Cytoplasmic foci are sites of mRNA decay in human cells. *J. Cell Biol.* 165:31–40. http://dx.doi.org/10.1083/jcb.200309008

Decker, C.J., D. Teixeira, and R. Parker. 2007. Edc3p and a glutamine/asparagine-rich domain of Lsm4p function in processing body assembly in *Saccharomyces cerevisiae. J. Cell Biol.* 179:437–449. http://dx.doi.org/10.1083/jcb.200704147

de Moor, C.H., and J.D. Richter. 1999. Cytoplasmic polyadenylation elements mediate masking and unmasking of cyclin B1 mRNA. *EMBO J.* 18:2294–2303. http://dx.doi.org/10.1093/emboj/18.8.2294

de Moor, C.H., H. Meijer, and S. Lissenden. 2005. Mechanisms of translational control by the 3′ UTR in development and differentiation. *Semin. Cell Dev. Biol.* 16:49–58. http://dx.doi.org/10.1016/j.semcdb.2004.11.007

Eulalio, A., I. Behm-Ansmant, D. Schweizer, and E. Izaurralde. 2007. P-body formation is a consequence, not the cause, of RNA-mediated gene silencing. *Mol. Cell. Biol.* 27:3970–3981. http://dx.doi.org/10.1128/MCB.00128-07

Flemr, M., J. Ma, R.M. Schultz, and P. Svoboda. 2010. P-body loss is concomitant with formation of a messenger RNA storage domain in mouse oocytes. *Biol. Reprod.* 82:1008–1017. http://dx.doi.org/10.1095/biolreprod.109.082057

Franks, T.M., and J. Lykke-Andersen. 2007. TTP and BRF proteins nucleate processing body formation to silence mRNAs with AU-rich elements. *Genes Dev.* 21:719–735. http://dx.doi.org/10.1101/gad.1494707

Franks, T.M., and J. Lykke-Andersen. 2008. The control of mRNA decapping and P-body formation. *Mol. Cell*. 32:605–615. http://dx.doi.org/10.1016/j.molcel.2008.11.001

Furuno, N., M. Nishizawa, K. Okazaki, H. Tanaka, J. Iwashita, N. Nakajo, Y. Ogawa, and N. Sagata. 1994. Suppression of DNA replication via Mos function during meiotic divisions in *Xenopus* oocytes. *EMBO J.* 13:2399–2410.

Gaffré, M., A. Martoriati, N. Belhachemi, J.P. Chambon, E. Houliston, C. Jessus, and A. Karaiskou. 2011. A critical balance between Cyclin B synthesis and Myt1 activity controls meiosis entry in *Xenopus* oocytes. *Development*. 138:3735–3744. http://dx.doi.org/10.1242/dev.063974

Gallouzi, I.E., C.M. Brennan, M.G. Stenberg, M.S. Swanson, A. Eversole, N. Maizels, and J.A. Steitz. 2000. HuR binding to cytoplasmic mRNA is perturbed by heat shock. *Proc. Natl. Acad. Sci. USA*. 97:3073–3078. http://dx.doi.org/10.1073/pnas.97.7.3073

Gebauer, F., and J.D. Richter. 1996. Mouse cytoplasmic polyadenylylation element binding protein: an evolutionarily conserved protein that interacts with the cytoplasmic polyadenylylation elements of c-mos mRNA. *Proc. Natl. Acad. Sci. USA*. 93:14602–14607. http://dx.doi.org/10.1073/pnas.93.25.14602

Groisman, I., Y.S. Huang, R. Mendez, Q.P. Cao, W. Theurkauf, and J.D. Richter. 2000. CPEB, maskin, and cyclin B1 mRNA at the mitotic apparatus: implications for local translational control of cell division. *Cell*. 103:435–447. http://dx.doi.org/10.1016/S0092-8674(00)00135-5

Hake, L.E., and J.D. Richter. 1994. CPEB is a specificity factor that mediates cytoplasmic polyadenylation during *Xenopus* oocyte maturation. *Cell*. 79:617–627. http://dx.doi.org/10.1016/0092-8674(94)90547-9

Hampl, A., and J.J. Eppig. 1995. Translational regulation of the gradual increase in histone H1 kinase activity in maturing mouse oocytes. *Mol. Reprod. Dev.* 40:9–15. http://dx.doi.org/10.1002/mrd.1080400103

Hochegger, H., A. Klotzbücher, J. Kirk, M. Howell, K. le Guellec, K. Fletcher, T. Duncan, M. Sohail, and T. Hunt. 2001. New B-type cyclin synthesis is required between meiosis I and II during *Xenopus* oocyte maturation. *Development*. 128:3795–3807.

Ihara, J., N. Yoshida, T. Tanaka, K. Mita, and M. Yamashita. 1998. Either cyclin B1 or B2 is necessary and sufficient for inducing germinal vesicle breakdown during frog (*Rana japonica*) oocyte maturation. *Mol. Reprod. Dev.* 50:499–509. http://dx.doi.org/10.1002/(SICI)1098-2795(199808)50:4<499::AID-MRD14>3.0.CO;2-Y

Kato, Y., and A. Nakamura. 2012. Roles of cytoplasmic RNP granules in intracellular RNA localization and translational control in the *Drosophila* oocyte. *Dev. Growth Differ.* 54:19–31. http://dx.doi.org/10.1111/j.1440-169X.2011.01314.x

Katsu, Y., M. Yamashita, H. Kajiura, and Y. Nagahama. 1993. Behavior of the components of maturation-promoting factor, cdc2 kinase and cyclin B, during oocyte maturation of goldfish. *Dev. Biol.* 160:99–107. http://dx.doi.org/10.1006/dbio.1993.1289

Kedersha, N., G. Stoecklin, M. Ayodele, P. Yacono, J. Lykke-Andersen, M.J. Fritzler, D. Scheuner, R.J. Kaufman, D.E. Golan, and P. Anderson. 2005. Stress granules and processing bodies are dynamically linked sites of mRNP remodeling. *J. Cell Biol.* 169:871–884. http://dx.doi.org/10.1083/jcb.200502088

Kloc, M., M.T. Dougherty, S. Bilinski, A.P. Chan, E. Brey, M.L. King, C.W. Patrick Jr., and L.D. Etkin. 2002. Three-dimensional ultrastructural analysis of RNA distribution within germinal granules of *Xenopus. Dev. Biol.* 241:79–93. http://dx.doi.org/10.1006/dbio.2001.0488

Kloc, M., M. Jaglarz, M. Dougherty, M.D. Stewart, L. Nel-Themaat, and S. Bilinski. 2008. Mouse early oocytes are transiently polar: three-dimensional and ultrastructural analysis. *Exp. Cell Res.* 314:3245–3254. http://dx.doi.org/10.1016/j.yexcr.2008.07.007

Knowles, R.B., J.H. Sabry, M.E. Martone, T.J. Deerinck, M.H. Ellisman, G.J. Bassell, and K.S. Kosik. 1996. Translocation of RNA granules in living neurons. *J. Neurosci.* 16:7812–7820.

Kondo, T., T. Yanagawa, N. Yoshida, and M. Yamashita. 1997. Introduction of cyclin B induces activation of the maturation-promoting factor and breakdown of germinal vesicle in growing zebrafish oocytes unresponsive to the maturation-inducing hormone. *Dev. Biol.* 190:142–152. http://dx.doi.org/10.1006/dbio.1997.8673

Kondo, T., T. Kotani, and M. Yamashita. 2001. Dispersion of cyclin B mRNA aggregation is coupled with translational activation of the mRNA during zebrafish oocyte maturation. *Dev. Biol.* 229:421–431. http://dx.doi.org/10.1006/dbio.2000.9990

Kosaka, K., K. Kawakami, H. Sakamoto, and K. Inoue. 2007. Spatiotemporal localization of germ plasm RNAs during zebrafish oogenesis. *Mech. Dev.* 124:279–289. http://dx.doi.org/10.1016/j.mod.2007.01.003

Kotani, T., and K. Kawakami. 2008. Misty somites, a maternal effect gene identified by transposon-mediated insertional mutagenesis in zebrafish that is essential for the somite boundary maintenance. *Dev. Biol.* 316:383–396. http://dx.doi.org/10.1016/j.ydbio.2008.01.043

Kotani, T., and M. Yamashita. 2002. Discrimination of the roles of MPF and MAP kinase in morphological changes that occur during oocyte maturation. *Dev. Biol.* 252:271–286. http://dx.doi.org/10.1006/dbio.2002.0853

Kotani, T., N. Yoshida, K. Mita, and M. Yamashita. 2001. Requirement of cyclin B2, but not cyclin B1, for bipolar spindle formation in frog (*Rana japonica*) oocytes. *Mol. Reprod. Dev.* 59:199–208. http://dx.doi.org/10.1002/mrd.1023

Kotani, T., S. Nagayoshi, A. Urasaki, and K. Kawakami. 2006. Transposon-mediated gene trapping in zebrafish. *Methods*. 39:199–206. http://dx.doi.org/10.1016/j.ymeth.2005.12.006

Kuersten, S., and E.B. Goodwin. 2003. The power of the 3′ UTR: translational control and development. *Nat. Rev. Genet.* 4:626–637. http://dx.doi.org/10.1038/nrg1125

Lécuyer, E., H. Yoshida, N. Parthasarathy, C. Alm, T. Babak, T. Cerovina, T.R. Hughes, P. Tomancak, and H.M. Krause. 2007. Global analysis of mRNA localization reveals a prominent role in organizing cellular architecture and function. *Cell*. 131:174–187. http://dx.doi.org/10.1016/j.cell.2007.08.003

Ledan, E., Z. Polanski, M.E. Terret, and B. Maro. 2001. Meiotic maturation of the mouse oocyte requires an equilibrium between cyclin B synthesis and degradation. *Dev. Biol.* 232:400–413. http://dx.doi.org/10.1006/dbio.2001.0188

Lin, M.D., X. Jiao, D. Grima, S.F. Newbury, M. Kiledjian, and T.B. Chou. 2008. *Drosophila* processing bodies in oogenesis. *Dev. Biol.* 322:276–288. http://dx.doi.org/10.1016/j.ydbio.2008.07.033

Mahowald, A.P. 1971. Polar granules of *Drosophila*. IV. Cytochemical studies showing loss of RNA from polar granules during early stages of embryogenesis. *J. Exp. Zool.* 176:345–352. http://dx.doi.org/10.1002/jez.1401760309

Malureanu, L., K.B. Jeganathan, F. Jin, D.J. Baker, J.H. van Ree, O. Gullon, Z. Chen, J.R. Henley, and J.M. van Deursen. 2010. Cdc20 hypomorphic mice fail to counteract de novo synthesis of cyclin B1 in mitosis. *J. Cell Biol.* 191:313–329. http://dx.doi.org/10.1083/jcb.201003090

Martin, K.C. 2004. Local protein synthesis during axon guidance and synaptic plasticity. *Curr. Opin. Neurobiol.* 14:305–310. http://dx.doi.org/10.1016/j.conb.2004.05.009

Downloaded from jcb.rupress.org on November 18, 2013

Published September 23, 2013

McGrew, L.L., E. Dworkin-Rastl, M.B. Dworkin, and J.D. Richter. 1989. Poly(A) elongation during *Xenopus* oocyte maturation is required for translational recruitment and is mediated by a short sequence element. *Genes Dev.* 3:803–815. http://dx.doi.org/10.1101/gad.3.6.803

Mendez, R., and J.D. Richter. 2001. Translational control by CPEB: a means to the end. *Nat. Rev. Mol. Cell Biol.* 2:521–529. http://dx.doi.org/10.1038/35080081

Nagahama, Y., and M. Yamashita. 2008. Regulation of oocyte maturation in fish. *Dev. Growth Differ.* 50(Suppl. 1):S195–S219. http://dx.doi.org/10.1111/j.1440-169X.2008.01019.x

Nakahata, S., Y. Katsu, K. Mita, K. Inoue, Y. Nagahama, and M. Yamashita. 2001. Biochemical identification of *Xenopus* Pumilio as a sequence-specific cyclin B1 mRNA-binding protein that physically interacts with a Nanos homolog, Xcat-2, and a cytoplasmic polyadenylation element-binding protein. *J. Biol. Chem.* 276:20945–20953. http://dx.doi.org/10.1074/jbc.M010528200

Nakahata, S., T. Kotani, K. Mita, T. Kawasaki, Y. Katsu, Y. Nagahama, and M. Yamashita. 2003. Involvement of *Xenopus* Pumilio in the translational regulation that is specific to cyclin B1 mRNA during oocyte maturation. *Mech. Dev.* 120:865–880. http://dx.doi.org/10.1016/S0925-4773(03)00160-6

Nakajo, N., S. Yoshitome, J. Iwashita, M. Iida, K. Uto, S. Ueno, K. Okamoto, and N. Sagata. 2000. Absence of Wee1 ensures the meiotic cell cycle in *Xenopus* oocytes. *Genes Dev.* 14:328–338.

Nakamura, A., R. Amikura, K. Hanyu, and S. Kobayashi. 2001. Me31B silences translation of oocyte-localizing RNAs through the formation of cytoplasmic RNP complex during *Drosophila* oogenesis. *Development*. 128:3233–3242.

Noble, S.L., B.L. Allen, L.K. Goh, K. Nordick, and T.C. Evans. 2008. Maternal mRNAs are regulated by diverse P body–related mRNP granules during early *Caenorhabditis elegans* development. *J. Cell Biol.* 182:559–572. http://dx.doi.org/10.1083/jcb.200802128

Novoa, I., J. Gallego, P.G. Ferreira, and R. Mendez. 2010. Mitotic cell-cycle progression is regulated by CPEB1 and CPEB4-dependent translational control. *Nat. Cell Biol.* 12:447–456. http://dx.doi.org/10.1038/ncb2046

Ota, R., T. Kotani, and M. Yamashita. 2011. Biochemical characterization of Pumilio1 and Pumilio2 in *Xenopus* oocytes. *J. Biol. Chem.* 286:2853–2863. http://dx.doi.org/10.1074/jbc.M110.155523

Parker, R., and U. Sheth. 2007. P bodies and the control of mRNA translation and degradation. *Mol. Cell*. 25:635–646. http://dx.doi.org/10.1016/j.molcel.2007.02.011

Pepling, M.E., J.E. Wilhelm, A.L. O'Hara, G.W. Gephardt, and A.C. Spradling. 2007. Mouse oocytes within germ cell cysts and primordial follicles contain a Balbiani body. *Proc. Natl. Acad. Sci. USA*. 104:187–192. http://dx.doi.org/10.1073/pnas.0609923104

Piqué, M., J.M. López, S. Foissac, R. Guigó, and R. Méndez. 2008. A combinatorial code for CPE-mediated translational control. *Cell*. 132:434–448. http://dx.doi.org/10.1016/j.cell.2007.12.038

Polanski, Z., E. Ledan, S. Brunet, S. Louvet, M.H. Verlhac, J.Z. Kubiak, and B. Maro. 1998. Cyclin synthesis controls the progression of meiotic maturation in mouse oocytes. *Development*. 125:4989–4997.

Sagata, N., I. Daar, M. Oskarsson, S.D. Showalter, and G.F. Vande Woude. 1989. The product of the mos proto-oncogene as a candidate "initiator" for oocyte maturation. *Science*. 245:643–646. http://dx.doi.org/10.1126/science.2474853

Salazar, A.M., E.J. Silverman, K.P. Menon, and K. Zinn. 2010. Regulation of synaptic Pumilio function by an aggregation-prone domain. *J. Neurosci.* 30:515–522. http://dx.doi.org/10.1523/JNEUROSCI.2523-09.2010

Schulte-Merker, S., R.K. Ho, B.G. Herrmann, and C. Nüsslein-Volhard. 1992. The protein product of the zebrafish homologue of the mouse T gene is expressed in nuclei of the germ ring and the notochord of the early embryo. *Development*. 116:1021–1032.

Seydoux, G., and A. Fire. 1994. Soma-germline asymmetry in the distributions of embryonic RNAs in *Caenorhabditis elegans. Development*. 120:2823–2834.

Sheets, M.D., C.A. Fox, T. Hunt, G. Vande Woude, and M. Wickens. 1994. The 3′-untranslated regions of c-mos and cyclin mRNAs stimulate translation by regulating cytoplasmic polyadenylation. *Genes Dev.* 8:926–938. http://dx.doi.org/10.1101/gad.8.8.926

Sheth, U., and R. Parker. 2003. Decapping and decay of messenger RNA occur in cytoplasmic processing bodies. *Science*. 300:805–808. http://dx.doi.org/10.1126/science.1082320

Stern, S., A. Rayyis, and J.F. Kennedy. 1972. Incorporation of amino acids during maturation in vitro by the mouse oocyte: effect of puromycin on protein synthesis. *Biol. Reprod.* 7:341–346.

Stutz, A., B. Conne, J. Huarte, P. Gubler, V. Völkel, P. Flandin, and J.D. Vassalli. 1998. Masking, unmasking, and regulated polyadenylation cooperate in the translational control of a dormant mRNA in mouse oocytes. *Genes Dev.* 12:2535–2548. http://dx.doi.org/10.1101/gad.12.16.2535

Swetloff, A., B. Conne, J. Huarte, J.L. Pitetti, S. Nef, and J.D. Vassalli. 2009. Dcp1-bodies in mouse oocytes. *Mol. Biol. Cell*. 20:4951–4961. http://dx.doi.org/10.1091/mbc.E09-02-0123

Tanaka, T., and M. Yamashita. 1995. Pre-MPF is absent in immature oocytes of fishes and amphibians except *Xenopus. Dev. Growth Differ.* 37:387–393. http://dx.doi.org/10.1046/j.1440-169X.1995.t01-3-00005.x

Tay, J., R. Hodgman, and J.D. Richter. 2000. The control of cyclin B1 mRNA translation during mouse oocyte maturation. *Dev. Biol.* 221:1–9. http://dx.doi.org/10.1006/dbio.2000.9669

Vassalli, J.D., J. Huarte, D. Belin, P. Gubler, A. Vassalli, M.L. O'Connell, L.A. Parton, R.J. Rickles, and S. Strickland. 1989. Regulated polyadenylation controls mRNA translation during meiotic maturation of mouse oocytes. *Genes Dev.* 3:2163–2171. http://dx.doi.org/10.1101/gad.3.12b.2163

Vessey, J.P., A. Vaccani, Y. Xie, R. Dahm, D. Karra, M.A. Kiebler, and P. Macchi. 2006. Dendritic localization of the translational repressor Pumilio 2 and its contribution to dendritic stress granules. *J. Neurosci.* 26:6496–6508. http://dx.doi.org/10.1523/JNEUROSCI.0649-06.2006

Yasuda, K., T. Kotani, R. Ota, and M. Yamashita. 2010. Transgenic zebrafish reveals novel mechanisms of translational control of cyclin B1 mRNA in oocytes. *Dev. Biol.* 348:76–86. http://dx.doi.org/10.1016/j.ydbio.2010.09.015

Zamore, P.D., J.R. Williamson, and R. Lehmann. 1997. The Pumilio protein binds RNA through a conserved domain that defines a new class of RNA-binding proteins. *RNA*. 3:1421–1433.

Zhang, B., M. Gallegos, A. Puoti, E. Durkin, S. Fields, J. Kimble, and M.P. Wickens. 1997. A conserved RNA-binding protein that regulates sexual fates in the *C. elegans* hermaphrodite germ line. *Nature*. 390:477–484. http://dx.doi.org/10.1038/37297

Zhang, Y., and M.D. Sheets. 2009. Analyses of zebrafish and *Xenopus* oocyte maturation reveal conserved and diverged features of translational regulation of maternal cyclin B1 mRNA. *BMC Dev. Biol.* 9:7. http://dx.doi.org/10.1186/1471-213X-9-7

Downloaded from jcb.rupress.org on November 18, 2013